

Universidad de Cádiz

**Proceso ecoeficiente sustitutivo del fresado químico  
de pieles metálicas aeronáuticas basado en  
tecnologías convencionales de mecanizado**

memoria presentada para optar al título de Doctor

Irene Del Sol Illana  
Septiembre 2019

Directores: Antonio Juan Gámez López  
Asunción Rivero Rastrero

University of Cadiz

**Eco-efficient process based on conventional  
machining as an alternative technology to chemical  
milling of aeronautical metal skin panels**

a dissertation submitted in partial fulfillment  
of the requirements for the degree of doctor of philosophy

Irene Del Sol Illana  
September 2019

Advisors: Antonio Juan Gámez López  
Asunción Rivero Rastrero

## Resumen

El fresado químico es un proceso diseñado para la reducción de peso de piezas metálicas que, a pesar de los problemas medioambientales asociados, se utiliza en la industria aeronáutica desde los años 50. Entre sus ventajas figuran el cumplimiento de las estrictas tolerancias de diseño de piezas aeroespaciales y que pese a ser un proceso de mecanizado, no induce tensiones residuales. Sin embargo, el fresado químico es una tecnología contaminante y costosa que tiende a ser sustituida. Gracias a los avances realizados en el mecanizado, la tecnología de fresado convencional permite alcanzar las tolerancias requeridas siempre y cuando se consigan evitar las vibraciones y la flexión de la pieza, ambas relacionadas con los parámetros del proceso y con los sistemas de utillaje empleados.

Esta tesis analiza las causas de la inestabilidad del corte y la deformación de las piezas a través de una revisión bibliográfica que cubre los modelos analíticos, las técnicas computacionales y las soluciones industriales en estudio actualmente. En ella, se aprecia cómo los modelos analíticos y las soluciones computacionales y de simulación se centran principalmente en la predicción off-line de vibraciones y de posibles flexiones de la pieza. Sin embargo, un enfoque más industrial ha llevado al diseño de sistemas de fijación, utillajes, amortiguadores basados en actuadores, sistemas de rigidez y controles adaptativos apoyados en simulaciones o en la selección estadística de parámetros. Además se han desarrollado distintas soluciones CAM basadas en la aplicación de gemelos virtuales.

En la revisión bibliográfica se han encontrado pocos documentos relativos a piezas y suelos delgados por lo que se ha estudiado experimentalmente el efecto de los parámetros de corte en su mecanizado. Este conjunto de experimentos ha demostrado que, pese a usar un sistema que aseguraba la rigidez de la pieza, las piezas se comportaban de forma diferente a un sólido rígido en términos de fuerzas de mecanizado cuando se utilizaban velocidades de corte cercanas a la alta velocidad. También se ha verificado que todas las muestras mecanizadas entraban dentro de tolerancia en cuanto a la rugosidad de la pieza. Paralelamente, se ha comprobado que la correcta selección de parámetros de mecanizado puede reducir las fuerzas de corte y las tolerancias del proceso hasta un 20% y un 40%, respectivamente. Estos datos pueden tener aplicación industrial en la simplificación de los sistemas de amarre o en el incremento de la eficiencia del proceso.

Este proceso también puede mejorarse incrementando la vida de la herramienta al utilizar fluidos de corte. Una correcta lubricación puede reducir la temperatura del proceso y las tensiones residuales inducidas a la pieza. Con este objetivo, se han desarrollado diferentes lubricantes, basados en el uso de líquidos iónicos (IL) y se han comparado con el comportamiento tribológico del par de contacto en seco y con una taladrina comercial. Los resultados obtenidos utilizando 1 wt% de los líquidos iónicos en un tribómetro tipo pin-on-disk demuestran que el IL no halogenado reduce significativamente el desgaste y la fricción entre el aluminio, material a mecanizar, y el carburo de tungsteno, material de la herramienta, eliminando casi toda la adhesión del aluminio sobre el pin, lo que puede incrementar considerablemente la vida de la herramienta.

## Agradecimientos

En primer lugar quiero agradecer a mis directores de tesis su guía y apoyo en estos cuatro años, gracias por vuestro tiempo invertido en continuas revisiones, reuniones y dudas. Gracias a Antonio por hacerte cargo de este proyecto pese a todas las adversidades, a Asun por estar siempre tan cerca pese a estar tan lejos, y a Mariano por embaucarme para entrar en esta aventura y cambiar mis objetivos completamente.

Gracias a Tecnia por ayudarme en todas las tareas experimentales, prestar su apoyo y sus medios. Especialmente tengo que agradecer a Antonio todo su trabajo y atención.

Gracias a la Universidad de Cádiz por el contrato predoctoral que ha permitido la financiación de la tesis, las ayudas de del plan Propio que han financiado la asistencia a congresos y las de movilidad UCA-Internacional que han financiado las dos estancias de investigación. Gracias al Departamento de Ingeniería Mecánica y Diseño Industrial por su apoyo y medios.

También quiero dar las gracias al grupo TEP-027. A Moi, Jorge y Juanma por los consejos, los ánimos y la motivación por probar cualquier locura. A Seve por arreglar cualquier equipo o situación que se me haya torcido, a Parra por disuadirme de empezar caminos sin salida y a Pedro por prestarse cada día y contagiarme su alegría. A Ale por escuchar tantas quejas y pesimismo y seguir queriendo quedar conmigo. A David por esos últimos ensayos. A los que empezaron casi a la par que yo Anapi, Fermín, Fran, Lucía, Luis y Sambruno, y a los que se han unido luego Magdalena, Rubén y Fernando, gracias por acompañarme en este camino.

Gracias a Miguel y a Luis por enseñarme a usar Python, hacer que mis gráficas sean “decentes y bonitas” y echar algún que otro cable con modelos y automatizaciones de trabajos de mono evitando que me volviera loca en más de un momento. También agradezco al grupo de corrosión por prestarse en cualquier momento frente a cualquier duda, especialmente a Juanito y a Marta.

Grazie a Fh-J\_LEAPT Naples per avermi accolto. In particolare a Cicio, per insegnarmi un po’ di Matlab et d’italiano. Grazie a tutti di DICMAPI per farmi sentire come a casa et grazie a Anto, Andrea e Dario per essere un sostegno anche al di fuori dell’università.

Thank you to the people in the Tribology-lab, Hong, Akshar, Akshey and the former member, Paarth, thank you to make my stay in Rochester so easy. Gracias a los españoles de RIT por esas comidas a las 12, y sobretodo, gracias Patricia por acogerme siendo tan cercana, por enseñarme no tener miedo a escribir un artículo y por abrirme un nuevo campo de conocimiento.

Gracias a mis padres, mi hermana y mi familia por el apoyo durante estos años. Gracias por vuestras oraciones y las de aquellos a los que se las habéis pedido. A Álvaro, por estar todos los días aguantándome, en las ausencias y los agobios y seguir a mi lado, sufriendo este tiempo a veces hasta más que yo. Finalmente, gracias, Dios.

## Contents

1. Abstract .....	3
2. Introduction and justification .....	3
3. Objectives and hypothesis .....	4
3.1. Objectives .....	4
3.2. Hypothesis .....	4
4. State of Art .....	4
4.1. Metal Skin Panels .....	4
4.2. Chemical Milling .....	5
4.3. Conventional milling alternatives .....	7
4.4. Ionic Liquids .....	7
5. Discussion .....	7
6. Conclusion .....	8
7. Perspectives .....	9
8. References .....	9
Appendix A: .....	13
Appendix B: .....	42
Appendix C: .....	57

## 1. Abstract

Chemical milling is a process designed to reduce the weight of metals skin panels. This process has been used since 1950s in the aerospace industry despite its environmental concern. Among its advantages, chemical milling does not induce residual stress and parts meet the required tolerances. However, this process is a pollutant and costly technology. Thanks to the last advances in conventional milling, machining processes can achieve similar quality results meanwhile vibration and part deflection are avoided. Both problems are usually related to the cutting parameters and the workholding.

This thesis analyses the causes of the cutting instability and part deformation through a literature review that covers analytical models, computational techniques and industrial solutions. Analytics and computational solutions are mainly focused on chatter and deflection prediction and industrial approaches are focused on the design of workholdings, fixtures, damping actuators, stiffening devices, adaptive control systems based on simulations and the statistical parameters selection, and CAM solutions combined with the use of virtual twins applications.

In this literature review, few research works about thin-plates and thin-floors is found so the effect of the cutting parameters is also studied experimentally. These experiments confirm that even using rigid workholdings, the behavior of the part is different to a rigid body at high speed machining. On the one hand, roughness values meet the required tolerances under every set of the tested parameters. On the other hand, a proper parameter selection reduces the cutting forces and process tolerances by up to 20% and 40%, respectively. This fact can be industrially used to simplify workholding and increase the machine efficiency.

Another way to improve the process efficiency is to increase tool life by using cutting fluids. Their use can also decrease the temperature of the process and the induced stresses. For this purpose, different water-based lubricants containing three types of Ionic Liquids (IL) are compared to dry and commercial cutting fluid conditions by studying their tribological behavior. Pin on disk tests prove that just 1wt% of one of the halogen-free ILs significantly reduces wear and friction between both materials, aluminum and tungsten carbide. In fact, no wear scar is noticed on the ball when one of the ILs is used, which, therefore, could considerably increase tool life.

## 2. Introduction and justification

Climate change and other environmental problems such as acid rain or water and air pollution could be reduced through more sustainable politics in transports and industry. The governments have passed laws worldwide to reduce the carbon emissions and increase the efficiency of the processes. Additionally, in a new global economy, the European industry compete with emerging countries that usually have lower salaries, less restrictive environmental and safety laws. Thus, the added value of European products should be their sustainability from the functional, social, economic and environmental point of view.

The aerospace industry is pioneer in this field including fuel efficiency of the product in their contract through the Target Weight of the airplane [1]. A reduction of their final weight has a direct impact on fuel consumption and consequently, on carbon emissions. To achieve it, one of the alternatives is to design the part by considering the minimum quantity of material needed to ensure its functional performance. Consequently, it is common to find parts -such as wings, doors or fuselages- with pockets in areas not subjected to loads.

Historically, these geometries are manufactured on metal skin panels through chemical milling. Double curvature parts are easy to manufacture using this technology, as it does not induce residual stresses and the clamping system is easy to implement. However, it is a slow and pollutant process where the waste treatment is costly and most of the chemicals are limited and tend to be banded. Since 2007, different research projects had studied conventional milling as an alternative technology

[2, 3]. Meanwhile complex clamping systems had been developed, few literature analyze the behavior of thin-plates or metal skin panels during the machining process. This type of machining is usually performed under dry conditions to avoid mineral oil-based lubricants and keep environmentally friendly parameters. Under this conditions, the efficiency of the process is usually reduced by the tool-life and the force increase. Therefore, new lubricants should be developed to ensure the sustainability of the process.

This thesis attempts to show research advances about thin-wall parts and thin-plates, analyzing the typical problems they presents such as vibrations and part deflection, and the different solutions provided during the last 20 years [4]. It also proves experimentally that machining may provide parts within the tolerances required in chemical milling, considering the effect of the cutting parameters on the final thickness and the roughness of the parts [5]. Additionally, the use of eco-friendly lubricants is proposed through a study of new water-based lubricant to improve the efficiency of conventional machining in terms of tool life and force efficiency [6].

### **3. Objectives and hypothesis**

#### *3.1. Objectives*

The main objective of the present work is to find a process more efficient and sustainable than the chemical milling.

In order to achieve it the specific objectives to pursuit are:

- O1. To establish the functional characteristics needed to ensure the performances of the skin panels and relate them to the surface integrity of the parts.
- O2. To correlate the milling parameters to the quality and performance requirements.
- O3. To select the most suitable parameters in order to compare the found process with the chemical milling.
- O4. To study the dynamic behavior of the system to define the conditions that ensure a stable machining process. This objective can be subdivided in:
  - Finding the parameters that ensure the correct performance of the part.
  - Modelling the dynamic behavior based on the frequency response of the system.

#### *3.2. Hypothesis*

In order to achieve these objectives, this thesis is based on four main hypothesis:

- H1. Conventional milling can be a sustainable alternative solution to chemical milling.
- H2. Conventional milling do not have any impact on the functional and quality requirements of the parts.
- H3. The performance of the metal skin panels can be studied through the surface integrity of the parts.
- H4. It is possible to correlate the milling parameters to the surface quality obtained in the sample parts.

### **4. State of Art**

The state of art is developed as a study of metal skin panels, chemical milling process, the milling process as a conventional alternative to manufacture low rigidity parts and the use of Ionic Liquids (IL) as eco-lubricants for machining. The state of art of thin-wall machining of light alloys [4] is one of the main contributions of this thesis and the complete text is included as the Appendix A.

#### *4.1. Metal Skin Panels*

Skin Panels are used as part of the airplanes fuselages, wings, doors, fan-cowls, etc. They are identified as the parts that cover the structure, reinforcing it and improving its aerodynamic [7,8]. They are also known as thin-floors or thin-plates parts by academics. Their low rigidity design is

combined with complex geometrical shapes where drills, pockets and profile contouring are needed to fit in the structure and to reduce its weight [9,10].

From a geometrical point of view, their thickness is usually between six and ten times lower than the other relevant dimensions [11] and the most common dimensional requirements are listed in **Table 1**.

The load supported in the thickness direction is usually negligible. However, the joining areas work as local tension points and they may present cracks and other similar failures. For this reason, the parts are specially designed to avoid fatigue behavior on the principal components of the load [12]. The material selected must have a high electrical conductivity to avoid its interaction with the avionics of the system and it should not be affected under the temperatures reached during the flight. Due to its properties, they are usually manufactured in aluminum, being the most common alloys Aluminum 7075-T6 and Aluminum 2024-T3. The first one is used for parts working under compression loads and, the second one for parts under fatigue loads [13].

**Table 1.** Typical dimensional requirements of skin panels.

Characteristic	Dimension (mm)	Tolerances (mm)	Reference
Pocket depth	1.60 to 6.35	±0.10 to ±0.13	[14] [2]
Pocket width	50 to 150	±0.15 to ±0.30	[14]
Pocket length	50 to 600	±0.15 to ±0.30	[13] [14]
Skin thickness	0.40 to 3.20	±0.05 to ±0.13	[15] [13]
Skin width	600 to 3000	-	[14]
Skin length	900 to 6000	-	[14]
Radius of curvature	600 to 1800	5%	[14]

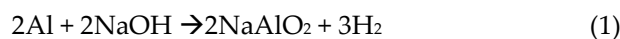
#### 4.2. Chemical Milling

Chemical milling was developed and patented by North American Aviation Inc. in 1953 to reduce rocket weights [16]. Its applications were extended to fuselages, turbines, rotors, shields and uniform aluminum foams [17]. The working flow of the process is shown in **Figure 1**.



**Figure 1.** Work flow of a general chemical milling process

Initially, the part is cleaned to improve the final tolerances and the surface quality obtained in the process. Later, the part is masked in a solution, resistant to the etching solution, to protect the areas that are not going to be machined. The typical materials used as maskant for different alloys are listed in **Table 2**. The maskant is scribed and removed in the areas selected to be machined. Then, the part is introduced in an acid or basic solution used as etching, different solutions and concentrations to use depending on the material can be found in **Table 3**. Particularly for aluminum alloys, the chemical reaction is described in equations (1) and (2) [18]. The time is controlled to ensure the final thickness of the part.



Finally, the part is rinsed and unmasked before quality control stages, where final thickness, roughness and process associated defects are verified. Tolerances achieved during this process can be between ±0.05 mm and ±0.3 mm and Roughness Average (Ra) is typically under 3.2 μm for



roughing and 1.6  $\mu\text{m}$  for accurate operations [19]. Process associated defects such as overhangs, dishing, channeling, ridging and filet notch are produced by the corrosion effect of the etchant, marks produced during the scribing step, non-homogeneous solutions and initial material properties [20]. The corrosion process have an effect on the fatigue performance of the part, reducing it by up to 50% compared to electro-etching process [21].

Furthermore, it should be considered that most of the chemicals used for half of the process steps –precleaning, masking, etching and pickling- are considerably pollutant. The metal removed from the part is solved into the etching, rising and pickling, forcing to treat the liquid wastes in a costly process [22]. These wastes also represent a health risk to the workers and have a negative impact on the environment.

**Table 2.** Masking for different materials [23]

Material	Masking
Aluminum Alloys	Polymers, neoprene, butyl rubber
Ferrous Alloys	Polymers, polyvinyl chloride, polythene and butyl rubber
Nickel Alloys	Neoprene
Magnesium Alloys	Polymers
Copper Alloys	Polymers
Titanium Alloys	Polymers
Silicon Alloys	Polymers

**Table 3.** Chemical milling solution for different materials. Removal rate between 0.3-0.5 mm/min. Adapted from [20].

Chemical Milling Solutions	Solution	Concentration (g/l)	Temperature (K)
Acid Based	Hydrochloric Acid <sup>1</sup>	2-3	303
	Aluminum Chloride <sup>2</sup>	50-80	320
	Hydrofluoric Acid	22-75	
	Hydrochloric Acid	26-42	
	Nitric Acid	111-300	303-322
	Oxalic Acid	0-0.8	
	Chromic Acid	30-53	
	Sulfuric Acid	165-225	305-352
Alkaline	Sodium Hydroxide <sup>3</sup>	136-280	344-380
	Sodium Gluconate <sup>3</sup>	0.3-3	344-380
	Sulfur <sup>3</sup>	7-8	344-380
	Sodium Sulfide <sup>3</sup>	8-9	344-380
	Triethanolamine <sup>3</sup>	20-60	344-380
	Sodium Polysulfide <sup>3</sup>	51-77	344-380
	Sodium Meta-aluminat <sup>4</sup>	120-140	
	Potassium Chromate <sup>4</sup>	30	
	Sorbitol <sup>4</sup>	2	
	Tributyl phosphate <sup>4</sup>	0.8-1	
	Carbomethylcellulose <sup>4</sup>	4	
	Thiourea <sup>4</sup>	1-2	

<sup>1</sup> Parameters for Aluminum serie 7045

<sup>2</sup> Parameters for Aluminum serie A92024

<sup>3</sup> Parameters for Aluminum series 2000, 6000 y 7000

<sup>4</sup> Special applications

#### 4.3. Conventional milling alternatives

Most of the studies of conventional milling as an alternative solution for chemical milling are focused on industrial applications. They usually design complex clamping systems that allow the machining of these thin parts by conventional milling. For example, Dufieux [24] and MTorres [25] developed mirror milling systems to ensure the minimum part deflection. Several studies [10,26,27] used virtual twins to ensure the position of the part in these type of machines, considering the real part geometry instead of the designed one. To reduce the scanning steps and the workholding cost, Mahmud et al. [28] presented a slave magnet system to reduce the cost of the machining and Rubio et al. [29] developed a flexible clamping system that varies the depth of cut using an adaptive control.

Nonetheless, conventional milling of skin panels has not been widely studied from the academic point of view. Thin-wall parts present similar behaviors during their machining to those obtained in thin-floors. Generally speaking, these low rigidity parts present several problems such as vibrations and part deflection during machining [30]. Different solutions had been proposed as analytics and computational models to statistical and workholding. They are summarized in the current state of the art that has been published on the journal "Materials" [4]. It is included in the thesis as Appendix A: *"Thin-Wall Machining of Light Alloys: A Review of Models and Industrial Approaches"*.

#### 4.4. Ionic Liquids

ILs are liquid salts, composed by organic cation and an inorganic anion, with a melting points below 100°C. They can be divided in Protic Ionic Liquids (PILs) and Aprotic Ionic Liquids (AILs). PILs are easier to synthesize and cheaper to produce but AILs have the ability to form hydrogen bonds which give them interesting properties [31]. Both types have low vapor pressure, high thermal stability, non-flammability and miscibility with polar phases, working as high performance lubricant [32] or as lubricant additives [33].

They are considered as an environmental alternative to mineral oils lubricant for several reasons [34]. They are able to reduce friction and wear in different pairs of contacts as metal-ceramic or metal-metal because in ILs are able to form a protective boundary film at the contact area [35]. Their physical adsorption is improved compared to other type of lubricant because of the polar nature of the ILs. Additionally, they have a low evaporation or decomposition rate, which reduce the environmental pollution, the quantity needed and the health impact.

Being tested for different applications, few research work in the machining field has investigated ILs as pure lubricant and as additive for Minimum Quantity Lubricants. Pham et al. [34] studied 1-ethyl-3-methylimidazolium bis(trifluoromethylsulfonyl)imide, and 1-butyl-3-methylimidazolium iodide, as pure lubricant for micro-machining application, improving the surface roughness obtained, and Davis et al. [36] tested 0.5wt% of 1-butyl-3-methylimidazolium hexafluorophosphate as an additive of a commercial MQL reducing the tool wear by up to 60%.

### 5. Discussion

The geometrical critical requirements for the most restrictive parts machined using chemical milling can be summarized as  $\pm 0.05$  mm dimensional thickness tolerance and roughness values below 1.6  $\mu\text{m}$ . The main difficulty to achieve them using conventional milling is the appearance of chatter, induced vibration and deflection produced by the cutting force effect. The literature review had shown that thin wall machining advances can be used to prevent chatter and deflection on thin-plate parts, especially by using analytical models, computational methods and parameter selection.

Experimental results had revealed that the feed rate did not affect the final depth of cut. Nonetheless, thermal expansion of the spindle had an influence on the final thickness that can be compensated by CAM, including spindle elongation as a function of the spindle speed. Cutting speed reduced the dispersion of thickness results. This dispersion was related to part vibration through a Fast Fourier Transform analysis. Higher spindle speed reduced the part vibration, having an effect into its oscillation in the thickness direction and obtaining a more stable machining in terms of

thickness. For the same reason, roughness values were lower with lower forces. The machining parameters seemed to have no other effect on surface quality.

Another relevant result is that according to Stability Lobes Diagrams, the clamping system thin-plate samples should provide a similar behavior to a rigid body. However, recorded forces in the axial direction presented lower values than the experiments performed in a rigid body, changing the main trend as the depth of cut changed. This variation is caused by the part stiffness that makes easier the reduction of the temperature, producing a similar behavior to high speed machining but within lower ranges of depth of cut.

Once the forces were characterized, they were modeled using Material Removal Rate (MRR) to measure the efficiency of the process and to correlate the forces to the cutting parameters. Higher speed reduced the temperature achieved and so the effort needed to cut the material, obtaining lower forces with higher quantities of MRR. Similarly, power consumption was modeled using statistical techniques. A statistical model correlating the theoretical consumption and the electrical consumption that could be useful as a low cost adaptive control was established.

Previous analysis showed that the better parameters to mill thin-plates are high cutting speed (up to 500 m/s) and medium-high feed rates (0.12 mm/teeth).

For the cases where high speed milling cannot be used, different lubricants based on ILs were tested. Its use could reduce the temperature reached, the forces needed and the induced residual stresses, improving the surface quality and the tool life. For this purpose, three different ILs were tested as an additive to water-based lubricant and compared to dry, water and commercial cutting fluid (CF) performance. One of the ILs was a halogen containing (Trihexyltetradecylphosphonium bis(trifluoromethylsulfonyl)amide [THTDP][NTf<sub>2</sub>]) and the other two were halogen free (Trihexyltetradecylphosphonium decanoate [THTDP][Deca] and Diethanol amine citrate Tri-[bis(2-hydroxyethylammonium)] citrate [DCI]).

[THTDP][NTf<sub>2</sub>] and [DCI] made no significant difference to water lubricating results. [THTDP][Deca] gave similar friction and wear values to the mineral oil cutting fluid tested. Wear values were related to the scar produced in the parts, being wider as the adhesion on the balls increased. This fact is produced by the change from aluminum-carbide to aluminum-aluminum, which also increase friction values and cutting forces whereas tests on [THTDP][Deca] improved the surface obtained and the energy consumption. They presented no wear on the ball and the wear tracks were small and clean, with no chemical variation between the wear track and the initial material. [THTDP][Deca] created a dynamic protection layer with low chemical affinity with the aluminum, while EDS results showed an increase on the oxygen inside the wear tracks for [DCI] and CF.

## 6. Conclusion

As a general conclusion it has been proved that, using the correct cutting parameters and workholding, conventional milling is a suitable alternative process to chemical milling using both dry and lubricating milling. Specific conclusion achieved in this thesis are listed below. They are classified by the works where they have been extracted.

*"Thin-Wall Machining of Light Alloys: A Review of Models and Industrial Approaches" [4]*

- The dynamic and the static problems produced by the low rigidity of the part are commonly related to the final quality of the part.
- Analytics models can be used to define the appearance of vibrations or deflection.
- Computational solutions must include mass loss and stiffness variation to provide an accurate solution but methods need to reduce computational time.
- Industrial approaches of thin-wall machining are mainly focused on the development of virtual twins, adaptive control and novel fixture systems to increase the efficiency of the process allowing more aggressive cutting parameters.

*“Effects of Machining Parameters on the Quality in Machining of Aluminum Alloys Thin Plates” [5]*

- Dimensional and roughness tolerances of the process are lower in conventional machining than in chemical milling, providing parts that fulfill the requirements
- Thin floors behave different from rigid bodies when high cutting speed parameters are used.
- Cutting parameters have an influence on the final thickness, surface roughness and cutting forces. Higher cutting speeds reduce the forces obtained in the z-axis, increase the stability of the process and reduce the tolerances of the process by up to 40% compared to conventional cutting speed. Lower values of forces ensure lower roughness results.
- Roughness meet the required tolerances using conventional milling if there is no chatter or vibrations.
- Final thickness can be adaptive controlled by the power consumption of the machine.

*“Tribological performance of ionic liquids as additives of water-based cutting fluids” [6]*

- Environmentally friendly lubricants can be used to increase tool life and reduce machining wastes.
- From the three tested ILs, [THTDP][Deca] is the most suitable one to be used as an additive to water-based lubricants in aluminum-carbide contact pairs.
- [THTDP][Deca] produces similar results as a halogen-containing commercial cutting fluid, reducing the friction coefficient compared to dry (75%) and water conditions (70%). It also reduces the wear track, improves its surface and removes the adhesion of aluminum on the carbide pin.

## 7. Perspectives

The results of this thesis support the idea that conventional milling is a sustainable alternative to chemical milling. Nonetheless, these findings provide the following insights for future research to make easier their efficiently implementation in the industry:

Further modelling work will have to be conducted in order to improve the accuracy of the results including stiffness variation and mass reduction in complex shape parts. New computational methods have to be developed to reduce the computational time.

Industry 4.0 technologies are still not implemented and its integration could increase skin panel milling profitability. Internet of things can be used to collect and treat data, establishing real time networks. Intelligent machine control can improve adaptive control systems. Metaheuristic algorithm analysis and machine learning could improve statistical models using big data analysis. Therefore, vibration and deflection control could be detected on-line.

Considerably more work will need to be done to determine the effect of fixture distance in the quality of the part. An in-depth study could simplify the workholding reducing the operation cost.

Large randomized controlled machining tests could provide more definitive evidence of the eco-friendly developed lubricant. Further research should be carried out to establish the effect of the cutting parameters, including ILs lubrication, on the residual stresses and corrosion behavior.

## 8. References

1. Salguero, J.; Fernandez-Vidal, S. R.; Mayuet, P.; Vazquez-Martinez, J. M.; Alvarez, M.; Marcos, M. Methodology for the Study of the Quality of CFRP Dry Drilling Based on Macrogeometrical and Dimensional Deviations. *World J. Eng. Technol.* **2016**, *04*, 200–205, doi:10.4236/wjet.2016.43D024.
2. Clean Sky 2 Novel manufacture of low weight skin without chemical milling-CS-GB-Written Procedure 2016-09 Amended WP & Budget 2016-2017 2017, 219–225.
3. Panczuk, R. Clean alternative technology to chemical milling: demonstration of technical, environmental and economic performance of mechanical milling for the machining of

complex shaped panels used in the aeronautical and space industries - GAP (Green Advanced Panel). *Layman Rep.* 2007.

4. Del Sol, I.; Rivero, A.; Norberto, L.; Gamez, A. J. Thin-Wall Machining of Light Alloys: A Review of Models and Industrial Approaches. *Materials (Basel)*. **2019**, *12*, 1–28.
5. Del Sol, I.; Rivero, A.; Gamez, A. J. Effects of Machining Parameters on the Quality in Machining of Aluminium Alloys Thin Plates. *Metals (Basel)*. **2019**, 1–11.
6. Del Sol, I.; Gámez, A. J.; Rivero, A.; Iglesias, P. Tribological performance of ionic liquids as additives of water-based cutting fluids. *Wear* **2019**, 426–427, 845–852, doi:10.1016/j.wear.2019.01.109.
7. Federal Aeronautical Regulations Aircraft Structure. In *Pilot Handbook*; pp. 1–16.
8. Dursun, T.; Soutis, C. Recent developments in advanced aircraft aluminium alloys. *J. Mater.* **2014**, *56*, 862–871, doi:10.1016/j.matdes.2013.12.002.
9. Zhou, G.; Li, Y.; Liu, C.; Hao, X. A feature-based automatic broken surfaces fitting method for complex aircraft skin parts. *Int. J. Adv. Manuf. Technol.* **2016**, 1001–1011, doi:10.1007/s00170-015-7774-y.
10. Hao, X.; Li, Y.; Deng, T.; Liu, C.; Xiang, B. Tool path transplantation method for adaptive machining of large-sized and thin-walled free form surface parts based on error distribution. *Robot. Comput. Integr. Manuf.* **2019**, *56*, 222–232, doi:10.1016/j.rcim.2018.10.007.
11. Scheider, I.; Brocks, W. Residual strength prediction of a complex structure using crack extension analyses. *Eng. Fract. Mech.* **2009**, *76*, 149–163, doi:10.1016/j.engfracmech.2008.06.035.
12. Bischoff, M.; Wall, W. A.; Bletzinger, K. U.; Ramm, E. *Encyclopedia of computational mechanics. Part 2: solids and structures*; Jonh Wiley & Sons, Ed.; Stein Erwin, de Borst René, Hughes Thomas JR: Chichester, UK, 2004;
13. Nui, M. C.-Y. *Airframe structural design: practical design information and data on aircraft structures*; 1st ed.; Conmilit Press Limited: Hong Kong, 1988; ISBN 962-7128-04-X.
14. Mahmud, A. Design of a Grasping and Machining edn Effector for Thin Aluminum Panel, École Polytechnique de Montréal, 2015, Vol. 1.
15. Menon, M.; Asada, H. Design and Control of Paired Mobile Robots Working Across a Thin Plate With Application to Aircraft Manufacturing. *IEEE Trans. Autom. Sci. Eng.* **2011**, *8*, 614–624.
16. M.C. Sanz Process of chemically milling structural shapes and resultant article 1956.
17. Matsumoto, Y.; Brothers, A. H.; Stock, S. R.; Dunand, D. C. Uniform and graded chemical milling of aluminum foams. *Mater. Sci. Eng. A* **2007**, *447*, 150–157, doi:10.1016/j.msea.2006.10.049.
18. Tomlinson, D.; Wichmann, J. Chemical Milling Environmental Improvements , Aerospace is Green and Growing. *NASF Surf. Technol. WHITE Pap.* **2014**, *78*, 1–7.
19. Rodriguez, V.; Nuñez, M.; Rodal, P. Fresado químico en el sector aeroespacial ventajas e inconvenientes. *IMHE* **2008**.
20. Totten, G. E.; MacKenzie, D. S. *Handbook of aluminum*; Dekker, 2003; ISBN 9780203912591.
21. Spear, A. D.; Ingraffea, A. R. Effect of chemical milling on low-cycle fatigue behavior of an Al-Mg-Si alloy. *Corros. Sci.* **2013**, *68*, 144–153, doi:10.1016/j.corsci.2012.11.006.
22. Çakir, O.; Yardimeden, A.; Özben, T. Chemical machining. *Achives Mater. Sci. Eng.* **2007**, *28*, 499–502.




23. El-Hofy, H. A.-G. *Advanced Machining Processes: Nontraditional and Hybrid Machining Processes*; 1st ed.; McGraw Hill Professional: United States, 2005; ISBN 0071466940.
24. Dufieux Dufieux Industrie - Modular Available online: <https://www.dufieux-industrie.com/en/products/mirror-milling-system-mms®> (accessed on Sep 10, 2019).
25. Mtorres Surface Milling Machining Available online: <http://www.mtorres.es/en/aeronautics/products/metallic/torres-surface-milling> (accessed on Sep 10, 2019).
26. Bao, Y.; Kang, R.; Dong, Z.; Zhu, X.; Wang, C.; Guo, D. Multipoint support technology for mirror milling of aircraft skins. *Mater. Manuf. Process.* **2018**, *33*, 996–1002, doi:10.1080/10426914.2017.1388519.
27. Bi, Q.; Huang, N.; Zhang, S.; Shuai, C.; Wang, Y. Adaptive machining for curved contour on deformed large skin based on on-machine measurement and isometric mapping. *Int. J. Mach. Tools Manuf.* **2019**, *136*, 34–44, doi:10.1016/j.ijmachtools.2018.09.001.
28. Mahmud, A.; Mayer, J. R. R.; Baron, L. Magnetic attraction forces between permanent magnet group arrays in a mobile magnetic clamp for pocket machining. *CIRP J. Manuf. Sci. Technol.* **2015**, *11*, 82–88, doi:10.1016/j.cirpj.2015.08.005.
29. Rubio, A.; Rivero, A.; Del Sol, I.; Ukar, E.; Lamikiz, A.; Rubio-Mateos, A.; Rivero-Rastrero, A.; Del Sol-Illana, I.; Ukar-Arrien, E.; Lamikiz-Mentxaka, A. Capacitation of flexibles fixtures for its use in high quality machining processes: An application case of the Industry 4.0 paradigm. *Dyna* **2018**, *93*, 608–612, doi:10.6036/8824.
30. Herranz, S.; Campa, F. J.; López de Lacalle, L. N.; Rivero, A.; Lamikiz, A.; Ukar, E.; Sánchez, J. A.; Bravo, U. The milling of airframe components with low rigidity: a general approach to avoid static and dynamic problems. *Proc. Inst. Mech. Eng. Part B J. Eng. Manuf.* **2005**, *219*, 789–801, doi:10.1243/095440505X32742.
31. Minami, I. Ionic Liquid Lubricants. *Encycl. Tribol.* **2013**, 1859–1866.
32. Matczak, L.; Johanning, C.; Gil, E.; Smith, T. W.; Schertzer, M. J.; Iglesias Victoria, P. Effect of cation nature on the lubricating and physicochemical properties of three ionic liquids. *Tribol. Int.* **2018**, *124*, 23–33, doi:10.1016/j.triboint.2018.03.024.
33. Jiménez, A. E.; Bermúdez, M. D. Short alkyl chain imidazolium ionic liquid additives in lubrication of three aluminium alloys with synthetic ester oil. *Tribol. - Mater. Surfaces Interfaces* **2012**, *6*, 109–115, doi:10.1179/1751584X12Y.0000000011.
34. Pham, M.-Q.; Yoon, H.-S.; Khare, V.; Ahn, S.-H. Evaluation of ionic liquids as lubricants in micro milling – process capability and sustainability. *J. Clean. Prod.* **2014**, *76*, 167–173, doi:10.1016/J.JCLEPRO.2014.04.055.
35. García, A.; González, R.; Hernández Battez, A.; Viesca, J. L.; Monge, R.; Fernández-González, A.; Hadfield, M. Ionic liquids as a neat lubricant applied to steel-steel contacts. *Tribol. Int.* **2014**, *72*, 42–50, doi:10.1016/j.triboint.2013.12.007.
36. Davis, B.; Schueller, J. K.; Huang, Y. Study of ionic liquid as effective additive for minimum quantity lubrication during titanium machining. *Manuf. Lett.* **2015**, *5*, 1–6, doi:10.1016/J.MFGLET.2015.04.001.

## **Appendix A:**

### *Thin-Wall Machining of Light Alloys: A Review of Models and Industrial Approaches*

Review

# Thin-Wall Machining of Light Alloys: A Review of Models and Industrial Approaches

Irene Del Sol <sup>1,\*</sup>, Asuncion Rivero <sup>2</sup>, Luis Norberto López de Lacalle <sup>3</sup> and Antonio Juan Gamez <sup>1</sup>

<sup>1</sup> Department of Mechanical Engineering and Industrial Design, Faculty of Engineering, Universidad de Cádiz, 11519 Puerto Real, Spain; antoniojuan.gamez@uca.es

<sup>2</sup> Tecnalia Research & Innovation. Scientific and Technological Park of Guipuzkoa, 20009 Donostia-San Sebastian, Spain; asun.rivero@tecnalia.com

<sup>3</sup> Department of Mechanical Engineering, University of the Basque Country, 48013 Bilbao, Spain; norberto.lzlacalle@ehu.eus

\* Correspondence: irene.delsol@uca.es; Tel.: +34956483513

Received: 28 May 2019; Accepted: 19 June 2019; Published: 23 June 2019



**Abstract:** Thin-wall parts are common in the aeronautical sector. However, their machining presents serious challenges such as vibrations and part deflections. To deal with these challenges, different approaches have been followed in recent years. This work presents the state of the art of thin-wall light-alloy machining, analyzing the problems related to each type of thin-wall parts, exposing the causes of both instability and deformation through analytical models, summarizing the computational techniques used, and presenting the solutions proposed by different authors from an industrial point of view. Finally, some further research lines are proposed.

**Keywords:** thin-wall machining; chatter; vibration; deflection; damping; prediction; workholding; fixture; dynamic; stability

## 1. Introduction

A wide range of aeronautical parts such as stringers, ribs, frames, spars, hubs, blisks, turbine blades, shells, bulkheads or skin panels can be classified as thin-wall structures [1]. They are designed to avoid mechanical assembly using bolts or rivets and to keep a uniform behavior all over the part. Thin-wall structures are usually manufactured out of advanced materials widely used in the aeronautical sector such as aluminum and titanium alloys, although some high-performance materials such as Inconel or specific types of stainless steel can also be used. Their good corrosion resistance and strength properties allow reducing the quantity of material needed, obtaining slim parts with a good weight–resistance ratio [2]. Therefore, thin-wall parts are manufactured by removing large quantities of material from the original block through a machining process, typically achieving a 30:1 buy-to-fly ratio [1]. The in-process parts are characterized by their low stiffness and constant change of mechanical properties. Their thickness is at least six times lower than the two other relevant directions, thus being flexible and easy to bend.

This fact produces dynamic and static problems during the machining operation. On the one hand, dynamic instabilities become frequent, and self-excited vibrations or chatter are more likely to appear, increasing the roughness of the final part, the tool wear and the wear of the different machine components [3,4]. Forced vibrations provoked by the dynamic of the machining operation also affect the final part, therefore reducing its quality. On the other hand, from a static point of view, both clamping and cutting forces produce elastic deformation that can affect the final dimension and the roughness of the part [5,6]. Induced residual stressed may also modify the final geometry of the part



during the process [7]. Additionally, preforms or skin panels have to be accurately positioned on the machining center to ensure the tight tolerances [8].

If these problems cannot be controlled, companies are forced to include reprocessing steps or discard useless parts, increasing the production cost. Being difficult to manufacture, thin-wall machining costs are justified just by weight reduction and fuel efficiency. For this reason, different organizations such as the European H2020 [9] have funded research projects on the improvement of thin-wall machining. Globally, this research line has been increasing, as can be appreciated by the number of papers focused on this topic published in international scientific databases (Figure 1).

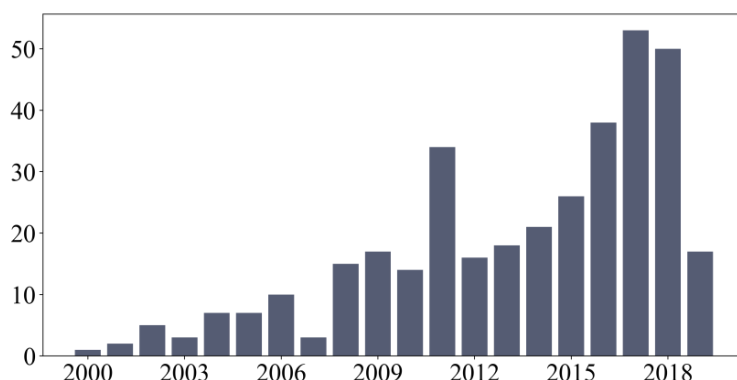


**Figure 1.** The number papers published on Web of Science related to thin-wall machining.

To ensure thin-wall quality, several authors have proposed analytical or computational dynamic models to predict the behavior of the part and select the best parameters to reduce chatter [10] or to damp the system [2]. Others have studied the deflection of the part due to the force interaction [11] or to the induced residual stress [12].

Alternatively, industry has developed special clamping or monitoring systems combined with adaptive control, such that quality is measured on-line and statistical parameters optimizations are used to monitor periodic changes [13].

The purpose of this work is to review the state of the art of thin-wall machining. Initially, thin-wall parts are identified, classified and associated to the critical problems previously introduced. Then, to understand the dynamic and static behavior of these machining operation, the most common analytics models are exposed. The proposed solutions, focused on models or industrial approaches, are explained in different sections and the reference distribution is summarized in Table 1. Finally, conclusions are drawn and possible future research lines are proposed.

**Table 1.** Thin-wall machining solutions. Model and industrial approaches.

Models		
Thin-wall dynamic problems	Chatter and self-exciting aspects	[14–42]
	Resonance and amplification	[33,41,43–60]
Thin-wall deformation	Quasi-static models	[36,49,61–70]
	FEM modeling	[51,61,62,65,71–78]
	Residual Stresses	[79–88]
Industrial Approach		
Parameter selection	Statistic and machine learning models	[62,89–95]
	Virtual Twins	[66,78,96–99]
Active solutions	Monitoring	[32,41,95,100–111]
	Measurements	[106,112–116]
	Fixtures	[83,116–126]
	Workholding	[19,75,127–131]
	Active damping actuators	[132–135]
	Stiffening devices	[136–140]

## 2. Type of Parts and Associated Problems

### 2.1. Thin-Wall Parts: Characteristics and Types

Thin-wall parts can include different types of parts, being their main characteristic their lack of stiffness and final slim factor, which is defined as their height divided by their thickness. Regarding the machining process and their characteristics, parts can be classified into two groups: monolithic blocks and skin panels.

Parts composing the first group have a geometry machined from monolithic blocks (Figure 2a–e). The part is obtained by removing a 90–95% of the initial material volume of the block by machining operations [141,142]. Stringers, ribs or frames are machined to obtain different pocket shapes, keeping their structural strength and reducing their weight. They are usually manufactured using three-axis machining, when the non-rigidity machining problems appear on the last steps for both, thin-floors and thin-walls. Impellers, blisks and blades are also included in this group, but their complex shapes require a constant change of the tool angle, changing the way the cutting forces are applied. Moreover, the cantilever produces a high deflection of the parts, making the control of the real depth of cut more difficult. Researchers use a sample part, represented in Figure 2e, as a simplification of the real cases to test and verify the machining parameters or to develop dynamic models reducing the computational time [143,144]. The behavior of the last roughing steps and end milling operation is then extrapolated to more complex shapes.

The other group, commonly known as skin panels, is mainly composed of shells, wings, fuselage parts (Figure 2g), bulkheads (Figure 2f), doors, satellite parts and frames, presenting a slim factor higher than ten [145]. Their buy-to-fly ratio is generally lower than those of monolithic parts. They are machined to pocket a large area of their surface, reducing the weight of the part. These pockets were traditionally machined using chemical milling, a highly pollutant process that does not induce residual stress and simplifies the clamping system [146]. However, since 2007, and mainly due to environmental reasons, special milling CNC centers have been designed and used for this purpose [147]. They are built with two symmetrical heads, hence the operation is named mirror milling. The machining head works perpendicular to the surface and a second head follows the machining head to ensure the support of the part and to reduce the deflection.

### 2.2. Dynamic and Static Problems

Generally, the main problem of thin-wall machining is the vibrations associated to their low rigidity. Depending on their cause, vibrations are considered self-induced (chatter) or forced.

Chatter takes place when the natural frequency response (FRF) of the system is excited due to the machining operation [14]. These instabilities are usually related to the tool vibrations produced during the machining but the most important one is the FRF of the part [17,25,27], which is constantly changing due to geometry variations. This cyclical behavior changes the FRF of the system and generates an unstable machining process [11,28]. Forced vibration or amplification takes place when the stiffness of the part is not enough to maintain a constant chip thickness. The workpiece and the tool deflect down to the edge action, producing a vibration at the same frequency as the spindle speed or multiples of it [32]. Both cases modify the contact between part and tool edge, changing the chip width, which affects the real cutting forces. Instabilities usually produce marks on the part that increase the roughness of the final product, affecting its final surface quality [45,60].

The other main problem associated to the low stiffness of the part is the dimensional error produced due to the deflection of the part, a static issue not considered on the machining of rigid parts. Machining of rigid parts usually deals with the flexibility of the cutter system [74], although it is not usually taken into account in traditional milling models. However, it is common to have an influence of the part and the cutting tool flexibility in thin-wall machining.

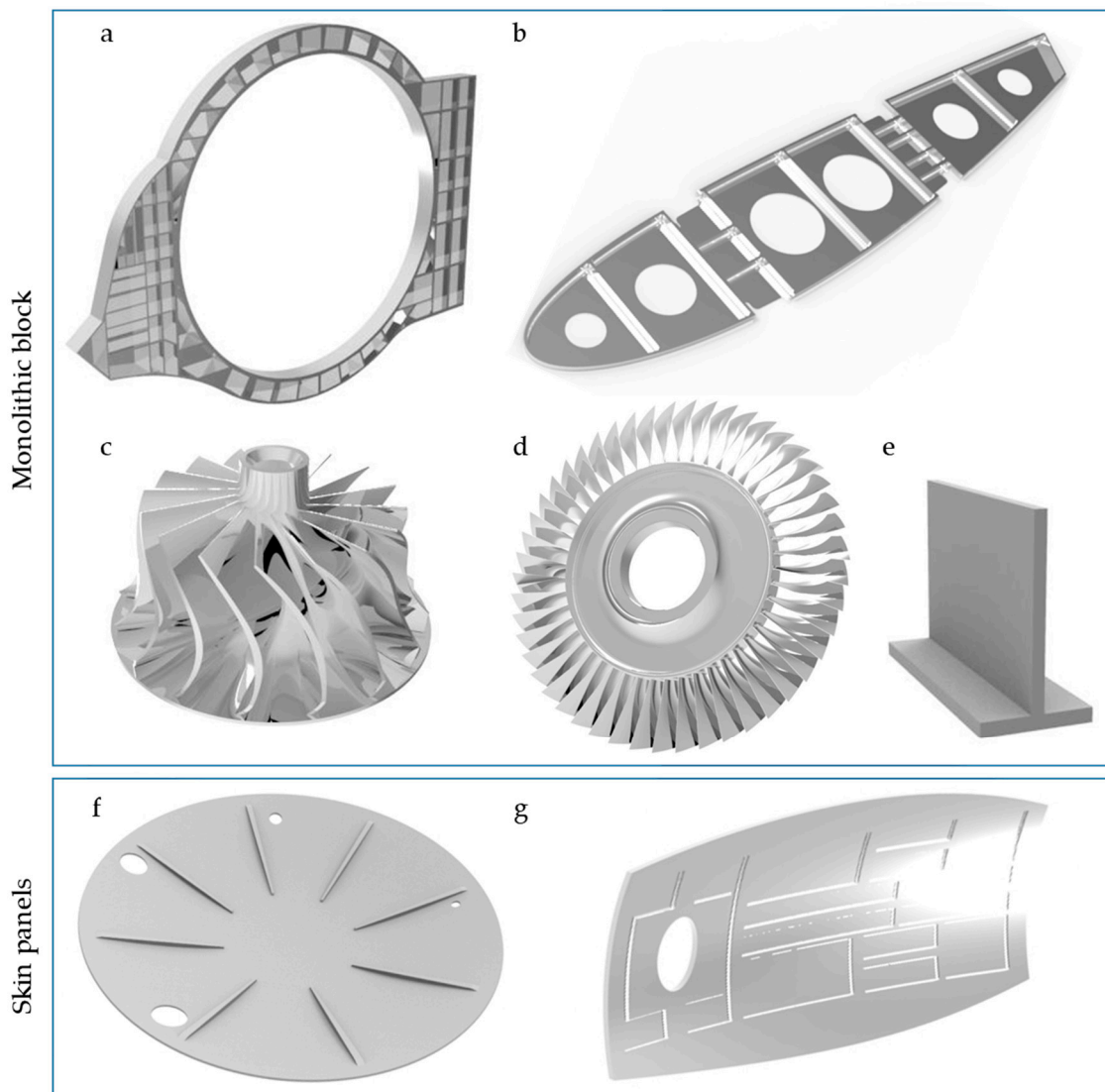


**Figure 2.** Examples of thin-wall parts: (a) frame; (b) rib; (c) impeller; (d) blisk; (e) sample parts; (f) bulkhead; and (g) fuselage skin.

Static deflection can appear due to the interaction of the cutting forces [63]. In this case, the deformation usually depends on the cutting strategy (up-milling or down-milling) and the cutting parameters, which define the cutting forces and, therefore, the deformation of the system [64,66–68,148]. Currently, high speed milling reduces cutting forces [2,10] and induces less residual stresses [7], but sometimes this technology cannot remove the deflection completely. This fact is aggravated in mirror milling due to the real part geometry variations [75,76]. Skins come from double curve processes and their position on the clamping system do not usually match the designed one, producing overcutting areas. Additionally, those parts are larger than the used in monolithic blocks, so the workholdings and fixtures do not usually ensure the tolerances of machining for the final parts and increase the difficulty of the whole machining process.

The different approaches found to predict and solve both issues are summarized in Figure 3, showing a complete work flow for thin-wall machining process. It covers the sequences used in physical and statistical models, commonly applied to improve the machining performance. For design and pre-industrialization stages, computational models and virtual twins allow selecting parameters or toolpath to reduce chatter and part deformation as well as to validate the design of specific work holding and stiffening devices. In industry, different workholding, stiffening devices or adaptive

control solutions based on statistics and machine learning models, have been developed following the outlines of industry 4.0.

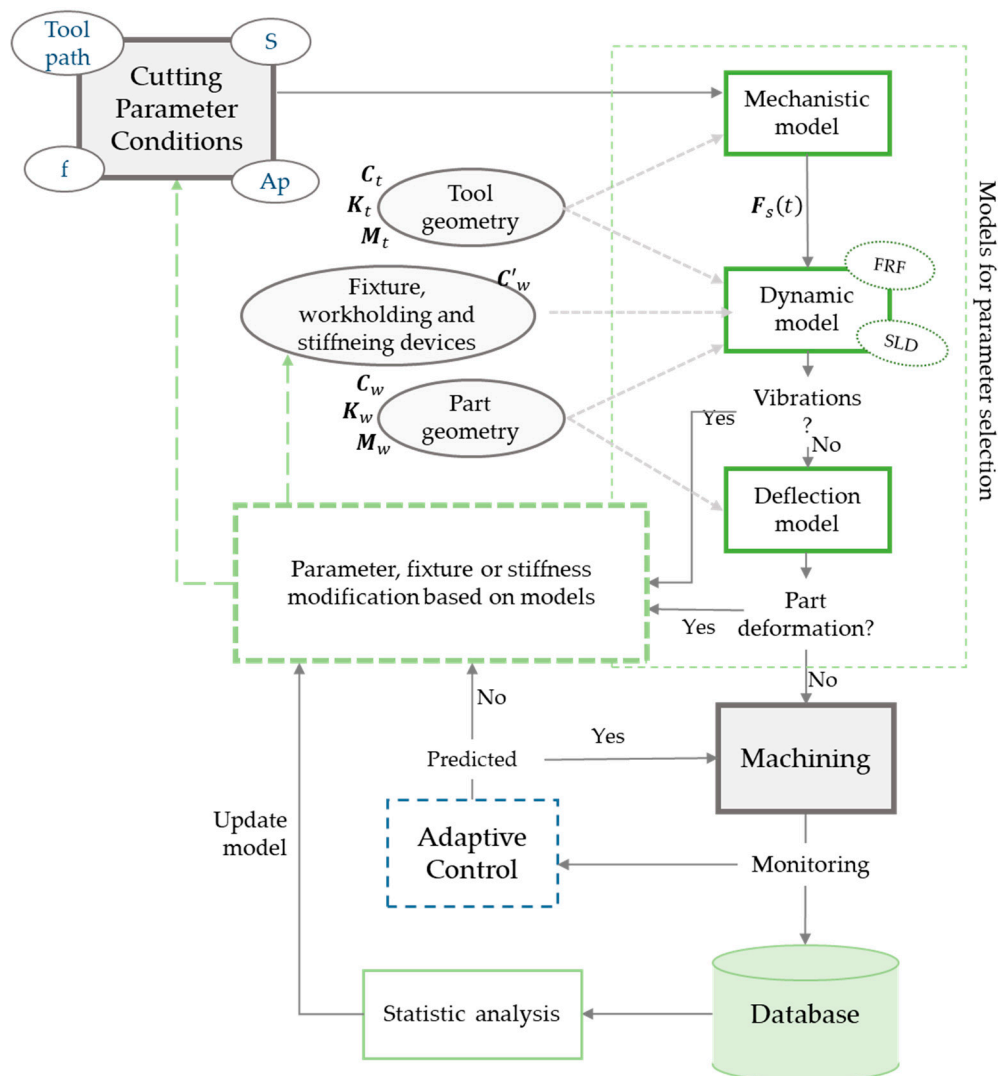


Figure 3. Scheme of the thin-wall machining process work flow.

### 3. Analytic Models

Dynamic response and machining performance of thin-wall parts were widely studied in the 1990s by Budak et al. [22,23]. Most of the research studies focused on the design of new methods to predict the behavior of the system are based on the FRF [57] and the deformations produced by the cutting forces [67]. Their final objective is the selection of the tool geometry and cutting parameters such that chip thickness is constant and vibrations are reduced. For this purpose, and to understand the physical fundamentals of thin-wall machining, analytic models of the forces, dynamics and deflection are explained in the following sections.

#### 3.1. Cutting Force Prediction

The expected forces can be calculated using a mechanistic model, which is adapted to the machining parameters, the tool, and the material as a function of the force coefficient. Tool geometry is very important, particularly to reduce vibration [1], and mechanistic models may be adapted to it. For this reason, Gradisek et al. [52] presented a generalization of the classical mechanistic model for most commercial tool geometries. Urbikain et al. [43,149] developed a specific model for a barrel tool shape,

in which the positioning angle of the tool and runout—eccentricity of the tool due to its positioning on the head spindle—is also considered. Ma et al. [44] performed a similar work including the relative position of the tool for five-axis applications and its effect on dynamic stability. In this section, the mechanistic model is described using a standard bull end mill (Figure 4a) considering also the tool angle position ( $\lambda$ ).

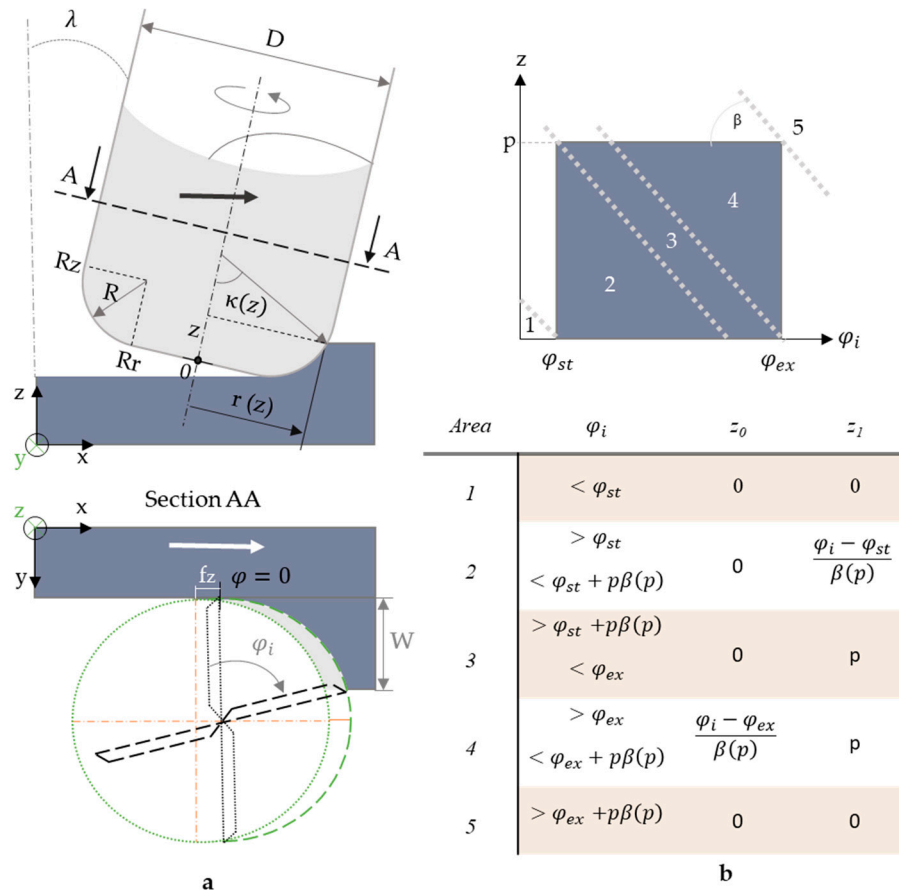


Figure 4. (a) Tool geometry; and (b) integration limits selection.

The force is obtained by integration of the differential edge elements contributing to the cut and summing the engaged teeth. The differential equation of the forces considering  $q = \{t, r, a\}$  as the component tangential, radial or axial, respectively, can be defined as:

$$\partial F_q(\varphi, z) = K_{qe} \partial S + K_{qc} h(\varphi, z) \partial b \quad (1)$$

where  $K_{qe}$  comprises the force coefficients related to the friction phenomena and  $K_{qc}$  the ones related to the cutting action.  $\partial b$  is the differential chip width and  $\partial S$  is the differential edge length.  $h$  is the chip thickness as a function of the rotated angle ( $\varphi$ ) and the axial depth of cut ( $z$ ).

$$\partial b = \frac{\partial z}{\sin \kappa(z)} \quad \partial S = \frac{\partial z}{\sqrt{1 - \left(\frac{R_a - z}{R}\right)^2}} \quad (2)$$

The instant rotation angle is defined as:

$$\varphi(\varphi_i, z) = \varphi_i - (j-1) \frac{2\pi}{N} - \beta(z) \quad (3)$$

where  $j$  is the teeth number from 0 to  $N$ , considering  $N$  the total number of teeth and  $\beta(z)$  the helix angle as a function of the instant depth of cut, and can be defined as:

$$\beta(z) = \left(1 - \frac{R_a - z}{R}\right) \tan \beta_0 \quad (4)$$

The instant chip thickness is defined as:

$$h(\varphi, z) = f_z \sin \varphi(\varphi_i, z) \sin \kappa(z) \sin \lambda \quad (5)$$

The integration limits are determined by the starting and ending angle of engagement of the tool and the  $z$  minimum ( $z_0$ ) and maximum ( $z_1$ ) values applied on the instant angle (Figure 4b).

Forces in Cartesian coordinates can be calculated including the position angle of the tool.

$$\frac{\partial F_{x,y,z}}{\partial z} = \begin{bmatrix} \sin \lambda & 0 & -\cos \lambda \\ 0 & 1 & 0 \\ \cos \lambda & 0 & \sin \lambda \end{bmatrix} \begin{bmatrix} -\cos \varphi & -\sin \varphi \sin \kappa & -\sin \varphi \cos \kappa \\ \sin \varphi & -\cos \varphi \sin \kappa & -\cos \varphi \cos \kappa \\ 0 & \cos \kappa & -\sin \kappa \end{bmatrix} \begin{bmatrix} \partial F_t \\ \partial F_r \\ \partial F_a \end{bmatrix} \quad (6)$$

Considering more than a single tooth, the total force applied is defined as:

$$F_{x,y,z}(\varphi_i) = \sum_{j=0}^N \left[ \int_{z_1}^{z_2} \partial F_{xyz,j}(\varphi_i, z) \right] \quad (7)$$

The accuracy of those models depends on the fitting used for the calculation of the force coefficients ( $K_{qc}$  and  $K_{qe}$ ), and they are commonly predicted through experimental tests. Coefficient values are considered constants for different feed rate per tooth ( $f_z$ ) while  $\partial b$  and  $\partial S$  depend on the tool geometry. The differential forces are studied on the Cartesian edges. Average forces for each test are used to calibrate the values of  $K_{qe}$  and  $K_{qc}$  for each condition of tool angle, material and spindle speed. Using at least two  $f_z$ , the six equations system is solved, obtaining the force coefficient. To improve the accuracy of the values, Liu et al. [105] used three spline interpolation. There are alternative methods to calculate  $K_{qc}$  and  $K_{qe}$  such as that of Du et al. [69], who used the Fourier form to determine the milling forces and then the force coefficient.

### 3.2. Dynamic Model

Once the cutting forces are calculated, stability of the system can be predicted based on the FRF and the cutting parameters values. To establish it, the degrees of freedom of the system are required. Tool and workpiece flexibility can be considered as independent, providing three different situations (Figure 5). The deflection of the part [10], the cutter system [64] or both [46] may affect the quality of the part in terms of final thickness and the roughness. For this reason, several researchers modeled the dynamic deformation of the system to predict the real quantity of material removed in each step and avoid reprocessing.

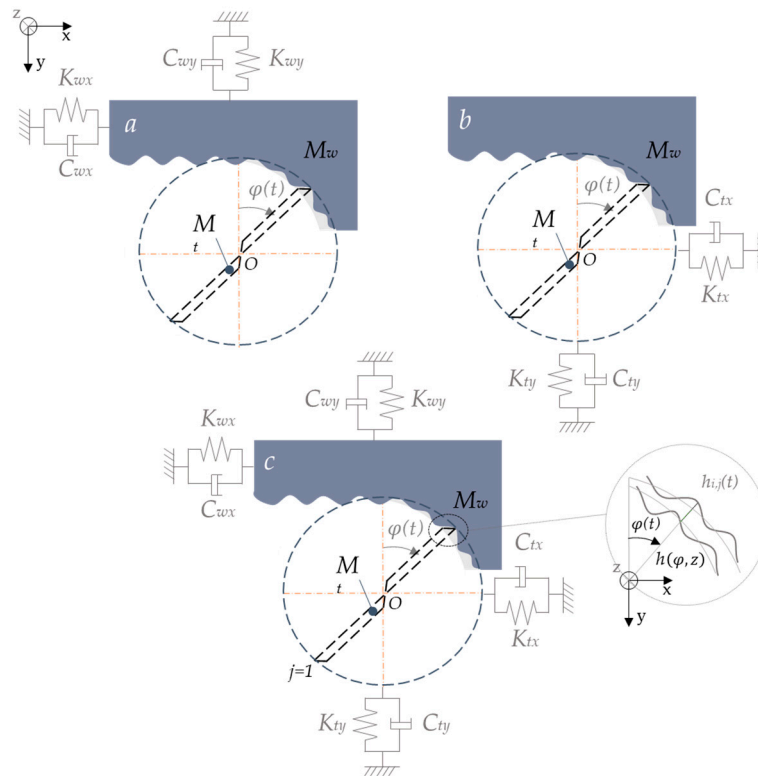


**Figure 5.** Flexibility of the system categorized as: (a) rigid cutter–flexible workpiece system; (b) rigid workpiece–flexible cutter system; and (c) double flexible system.

Most studies are based on the following assumptions:

- Temperature and other factors related to the machining process do not affect the behavior of the tool and the workpiece during the cutting operation.
- The only force considered is the cutting force, and deformation is only elastic.

Considering a mixed situation and a multiple contact model, the dynamic behavior of the system can be modeled by an equation of the form:

$$M_s \ddot{Q}_s(t) + C_s \dot{Q}_s(t) + K_s Q_s(t) = F_s(t) \quad (s = w, t) \quad (8)$$

where mass ( $M_s$ ), damping ( $C_s$ ) and stiffness ( $K_s$ ) are matrices with dimension  $3n_s \times 3n_s$  on the workpiece ( $w$ ) and the tool ( $t$ ). The vibration vector  $Q_s(t)$  is defined by the modal displacement ( $\Gamma_s(t)$ ) and the mass normalized mode ( $U_s$ ).  $\zeta_s$  is the modal damping ratio matrix and  $\omega_s$  is the diagonal FRF matrix, both matrices having the dimension of  $m_s \times m_s$ .

$$\ddot{\Gamma}_s(t) + (2\zeta_s \omega_s) \dot{\Gamma}_s(t) + \omega_s^2 \Gamma_s(t) = U_s^T F_s(t) \quad (9)$$

where

$$\Gamma_s(t) = \begin{Bmatrix} \Gamma_t(t) \\ \Gamma_w(t) \end{Bmatrix}, \quad \omega_s = \begin{bmatrix} \omega_t & 0 \\ 0 & \omega_w \end{bmatrix}, \quad \zeta_s = \begin{bmatrix} \zeta_t & 0 \\ 0 & \zeta_w \end{bmatrix}, \quad U_s = |U_t - U_w|, \quad (10)$$

$$F_s = F_t = -F_w \quad (11)$$

$F_s(t)$  correspond to the cutting forces and is calculated following the force prediction section but, in this case, chip thickness ( $h_{i,j}$ ) and axial immersion angle ( $\kappa$ ) should consider the dynamic interaction:

$$h_{i,j}(t) = [x_{i,j}(t) - x_{i,j}(t - T_{j-1})] \sin \varphi(t) + [x_{i,j}(t) - x_{i,j}(t - T_{j-1})] \cos \varphi(t) \quad (12)$$



$$\kappa(t) = \cos^{-1}\left(\frac{\mathbf{V} \cdot \mathbf{P}}{|\mathbf{P}|^2 |\mathbf{V}|}\right) \quad (13)$$

$x$  and  $y$  are the displacement between tool and workpiece during the effect of the  $j$  cutting flute at the time interval  $t$ .  $T_{j-1}$  is the time interval between two following flutes.  $\mathbf{V}$  is the tool axis vector and  $\mathbf{P}$  is the relative position vector to the instant  $t$ , both of which depend on the instant relative position between the part and the tool (Figure 6).

$$\mathbf{V} = (V_x, V_y, V_z) \quad \mathbf{P} = (x_0 - x_{i,j}(t), y_0 - y_{i,j}(t), z_0 - z_{i,j}(t)) \quad (14)$$

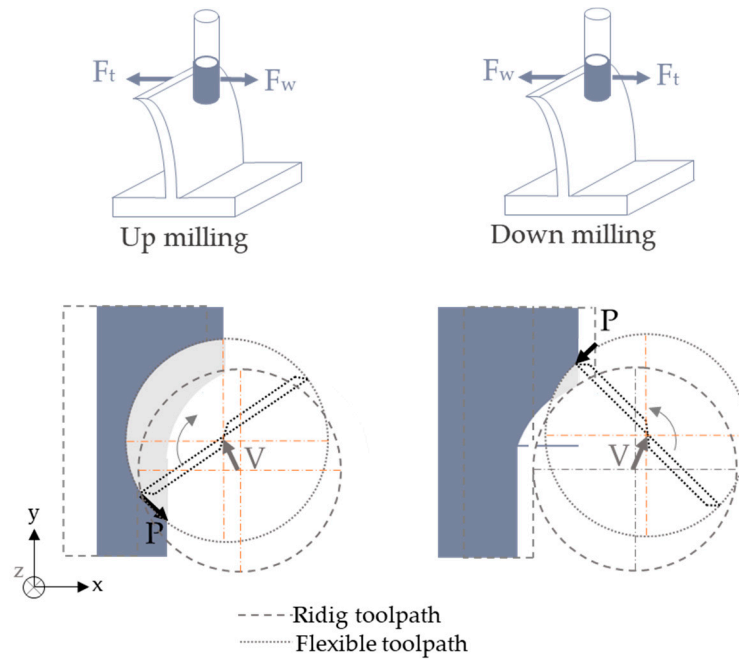


**Figure 6.** Deflection produced on the parts considering displacement of workpiece and tool.

### 3.3. Deflection Model

Once the forces are stable and no chatter appears, deflection can still produce over cutting or under cutting. The normal force applied to the part can bend it depending on its stiffness ( $k$ ), producing a displacement ( $\delta$ ) of the contact point between the workpiece and the tool.

$$F = k \delta \quad (15)$$

Fixing the deflection,  $F$  can be related to the thickness of the part (Figure 7). The maximum value of the force is determined by the Young's modulus ( $E$ ), the Poisson ratio ( $\mu$ ), the position of the tool, and the total thickness ( $w$ ). This thickness should be corrected considering the addendum to the real thickness depending on the location ( $\Delta w(u, v)$ ), based on the tool referenced axis, and considering the residual thickness over the designed surface [66]. The final displacement is obtained based on the predicted forces. This model can be applied not only to cantilever plates but also to more complex geometries.

$$F = \frac{E}{(1 - \mu^2)} f(a, b, c) (w + \Delta w(u, v))^3 \quad (16)$$



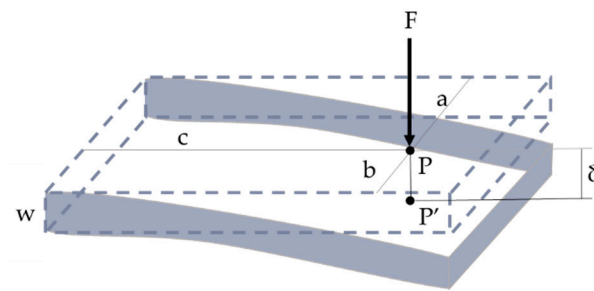


**Figure 7.** Scheme of the bending of thin-wall produced by the cutting forces.

#### 4. Computational Solutions

Computational analysis is used for the study of the final behavior of the part. It analyzes and predicts the vibration and deflection behavior during thin-wall milling. In both cases, initial forces are calculated using mechanistic models based on experimental data [64] or commercial software such as AdvanEdgeTM [70], VERICUT® [148] or DEFORMTM [77]. They are used as inputs for the initial conditions of the workpiece. Then, self-developed or commercial software such as ANSYSTM [20,24,34,71] or ABAQUS [29,35,53,58,71,150] are used to obtain the FRF of the system, the dynamic behavior or its deflection.

##### 4.1. Vibration Prediction

Different authors tried to establish new dynamic models based on computational experiments in order to predict chatter or forced vibrations during the machining of thin-wall parts. Most of them are based on the study of the FRF by analyzing Stability Lobes Diagrams (SLD) and instant chip engagement to choose the correct cutting parameters in order to improve surface quality of the part and reducing tool wear [21].

##### 4.1.1. Chatter

Chatter prediction starts by calculating the FRF of the workpiece and tool-spindle using impact hammer test [15,26,30,31,36–38]. One point of the tool and different locations of the workpiece are hit, and excitation responses are recorded by accelerometers. The weight of the accelerometers is subtracted from the total weight of the system. The data are treated and filtered to determine the FRF matrix and the modal damping ratio matrix. Damping ratios are usually considered constant during milling and FRF be studied under the most critical situations [3].

Those results lead to a general dynamic model that is dependent on the machining parameters. As is well known, machining parameters directly affect the efficiency of the process and, in this particular case, its stability. To ensure both of them, most researchers study the SLD of the system.

SLD are one of the most common tools used in thin-wall machining to select parameters in order to reduce chatter by just setting the correct machining parameters in terms of efficiency [39–41]. SLD usually represents the stability areas based on the axial depth of cut and the spindle speed (Figure 8). However, typical methods for calculating SLD determine more restrictive areas than they should [40,46]. This is the reason recent works focus on the improvement of its calculation.

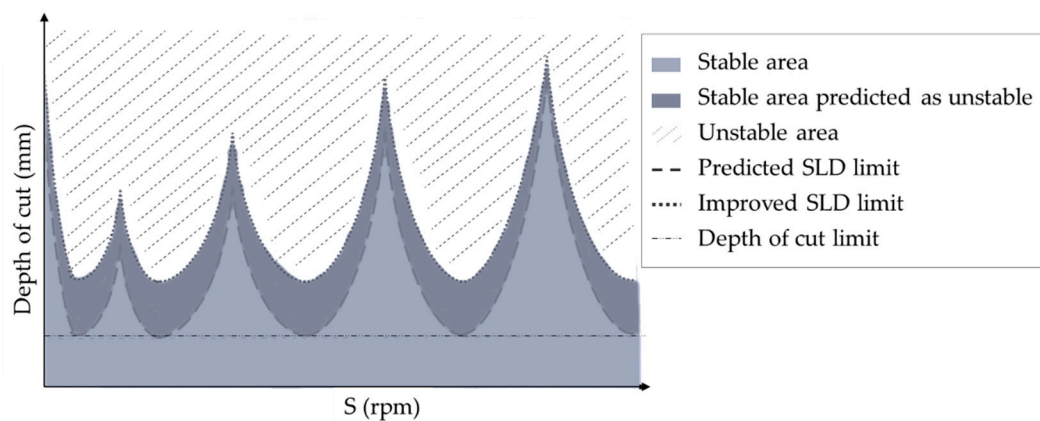


**Figure 8.** Schematic SLD presenting stable and unstable areas and the possible improvement of the SLD limit curve.

Several authors [25,30,42,150] considered more than one parameter machining condition, generating 3D-SLD. Their studies mainly focus on sample parts to generalize monolithic part machining behavior. For instance, Olvera et al. [39], Germashev et al. [40] and Guo et al. [16] studied the runout and helix angle effect in a SLD, while Urbikain et al. [149] and Jing et al. [20] compared the effect of the tool position. Liu et al. [105] focused their research in the effect of the radial depth of cut and Qu et al. [25] analyzed the feed rate effect. Feng et al. [18] evaluated the effect of velocity-dependent mechanisms to obtain a closer SLD, obtaining better results than the ones using a plowing force coefficient. Finally, some studies are focused on the fixture effect, such as the flexible support [46] or the damping system [19,31,47].

However, few works were found where SLD approach is applied to mirror milling applications or similar test combinations [15,20]. For those cases, bull and ball end mills are used to analyze the effect of the angle or relative position of the tool in the SLD [15].

#### 4.1.2. Amplification

Resonance and amplification can be predicted based on the differential equations of the dynamic behavior of the system, which can be calculated through semi-analytical methods. These models have usually been developed in MATLAB [25,48,49] or C++ [45]. However, this solution is time consuming and has low accuracy. For this reason, one of the most recent approaches is to develop more efficient ways to solve the stability differential equations. Song et al. [50] used the Sherman–Morrison–Woodbury formula to calculate FRF considering the mass loss, whereas Li et al. [64] used a Runge–Kutta method for the same purpose. Feng et al. [18] used Taylor series to linearize the dynamic equations and Olvera et al. [39] solved the model using enhanced multistage homotopy perturbation (EMHP) and Chebyshev method in order to improve the accuracy.

Other authors use computational methods to predict vibrations. In this case, it is important to consider mass loss and tool wear because they can also modify the dynamics of the system and thus the stability of the machining [51]. This consideration implies a constant remeshing and reanalysis, involving a considerable computing time. Some authors tried to include the effect of the material loss. Meshreki et al. [151] proposed the use of 2D multispan plate (MSP). It improved the computational efficiency but it can only be applied to simple geometries. Budak et al. and Yang et al. [21,33] developed Structural Dynamic Modification (SDM) by updating the mass loss by the time domain. Tuysuz and Altintas [57] developed an iterated improved reduction system technique combined with a matrix perturbation technique to use the computational time only once. Yang et al. [29] used component mode synthesis (CMS) and space structural modification to develop a decomposition-condensation model that reduce computational time. Fei et al. [20] solved the dynamic model using a semi-discretization method. Ding et al. [19] established a dynamic model dividing the part and analyzing the FRF on both

parts. Li et al. [64] improved roughness by developing a dynamic model for machining of integral impellers blades. Shuang et al. [59] used a coupled Eulerian–Lagrangian model to relate the chip formation to the cutting forces oscillation amplitudes, reducing the surface roughness produced by part deformation. The model used by Tian et al. [26] is presented as a theoretical base for suppressing resonance in the milling process. Ahmadi [55] compared a Finite Strip Model (FSM), FEM analysis and a semi-analytical model for the study of the dynamics of thin-wall machining (Figure 9). Lin et al. [56] studied the FRF of the machining system and related the waviness of the part with the force vibrations and not to the self-excited vibrations.

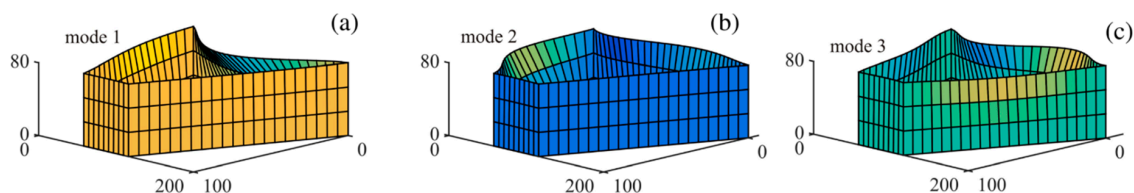


**Figure 9.** Average deflection obtained for (a) the first mode, (b) the second mode and (c) the third mode of a pocket structure [55].

#### 4.2. Dimensional Error Prediction

Computational methods for part deflection analysis usually involve simulations to estimate deflection of the part and reduce the dimensional tolerances of the process neglecting the dynamic response of the system [61].

Initially, the applied force is calculated based on mechanistic models and considering the instant chip formation. To improve the accuracy of the model, approaches such as the finite difference method are employed only for the contact interference between workpiece and tool [34] or Eulerian–Lagrangian methods to predict the chip formation and the final force applied [74].

Generally, the workpiece material is modeled using the Johnson–Cook law [74,78] and elastoplastic behavior should be considered [5]. Residual stress can be excluded from the material model since the induced residual stresses are more significant than those produced by previous forming steps such as rolling or forging [65]. However, their effect should be taken into account to predict the final part deflection.

The workpiece deflection is predicted through iteration and considering a quasi-static situation [61,70]. The analysis is performed following the toolpath and iteration must be performed for every new tool position due to the change of the workpiece–tool contact and the workpiece stiffness. In fact, the deformation produced by these changes can vary considerably just in one rotation of the spindle, as illustrated in Figure 10. Consequently, for each new position, the part should update the existing material, remeshing the workpiece and considerably increasing the computing time. Izamshah et al. [142] combined FEM and statistical models to reduce it in the simulation of the surface error. Ratchev et al. [62] addressed the solution by using a volume element-based surface generation approach to predict the deflection of the part. Similarly, Si-meng et al. [72] increased the solving speed by changing the simulation method. They considered the material loss using Boolean operations and hexahedral mapping algorithms, including tool and workpiece springback. Their models were validated with an error lower than 15%. Wang and Si [49] discarded the mesh subdivision or mesh adaptive technology because both considerably increased the computational burden, whereas the accuracy was not improved. Meanwhile, they simulated stiffness variation by removing the two elements adjacent to the cutter location, improving deflection accuracy.

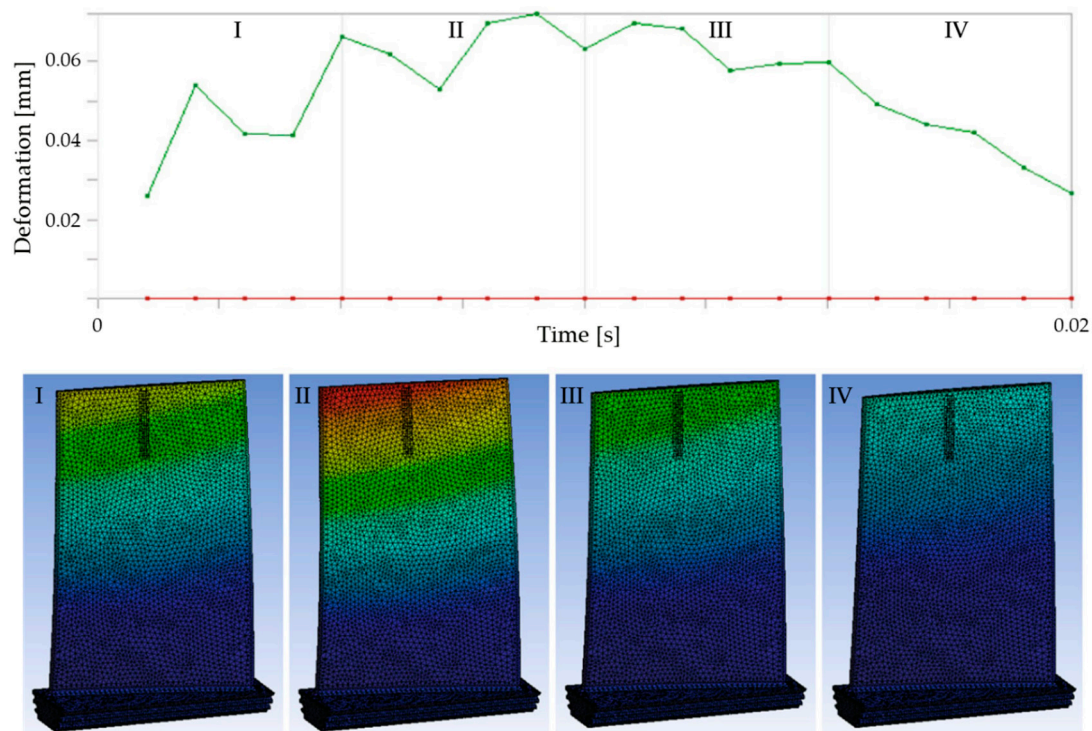


**Figure 10.** Deformation of a blade during one period rotation of the spindle [78].

Other authors focused on how the parameters affect the deflection of the part. Some of them studied the effect of the wall thickness [67,73], the depth of cut [66] or the feed rate [61,78] on the dimensional error. Others authors considered the tool position [49,70] and the fixture system [5]. Zhang et al. [28] went further by including the effect of the distance to the clamping system.

Another factor to take into account in the final dimensional error is the induced residual stress. It is usually evaluated for thin-walled parts through X-ray [79–82], neutron diffraction [83] or XDR [84] technologies. Residual stress can be affected by the cutting parameters, such as tool geometry [81,82], depth of cut [79], final quality, tool path [65], process temperature [84] and cutting forces [84]. In fact, the selection of the proper parameters with the aim of reducing the induced residual stress can lower the part deflection up to 45% [85]. For instance, Masoudi et al. [84] proved the effect of high-speed machining conditions on the reduction of the distortions produced by residual stresses, considering also that an increase of the depth of cut would increase the internal stress. Gao et al. [86] proposed a semi-analytical method to predict the deformation of thin-wall machining parts based on the effect of the residual stress present on the part. Jiang et al. [81,82] studied the uncut chip thickness effect on the induced residual stresses, relating also the strategy—up or down milling—and the change of tool diameter.

Once the deflection is predicted, many methods apply the results to compensate the tool path or to modify the cutting parameters in order to reduce it [62]. Hao et al. [87] used this approach to correct blade deflections and to geometrically predict the roughness of the final part produced by the separation between the workpiece and the tool. Chen et al. [6] reduced the final error by applying a toolpath compensation strategy. Richter-Trummer et al. [12] presented a simulation method that predicted the distortion produced by residual stresses and allowed managing it, ensuring the dimensional quality of the machining parts. Similarly, Wu et al. [88] used quasi-symmetric machining to reduce the deformation produced by residual stresses. The machining results are considerably more accurate when the compensation is made at the last layer (Figure 11).

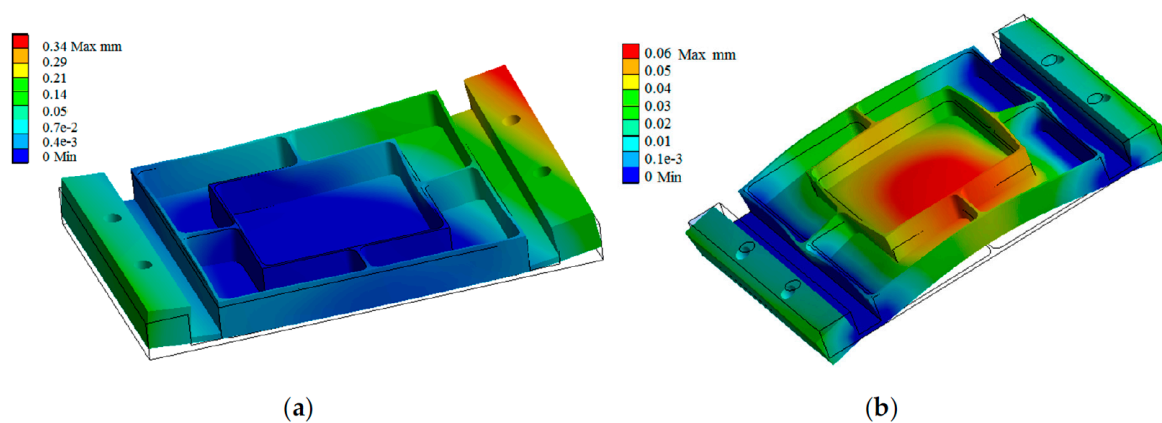


**Figure 11.** Deformation of a thin-wall part: (a) not considering the residual stress; and (b) following a quasi-symmetric machining reducing the residual stress [88].

## 5. Industrial Approach

Apart from computational modeling, several solutions following an industrial approach have been developed such as parameter selection, adaptive control, or workholdings and fixture design.

### 5.1. Parameters Selection

Parameter selection can be established through experimental data-based models, commonly statistics or neural network based models, or through virtual twins studies, in which depth of cut and toolpath are modified to ensure the final thickness of the part.

#### 5.1.1. Database Models

Cutting parameters for thin-wall machining are also studied from an experimental and statistical point of view [13,89–94]. Researchers developed experimental models based on ANOVA results by analyzing how the cutting parameters and machining strategies affect the roughness and the dimensional error. Sonawane et al. [89] used ANOVA analysis to reduce the deflection of a cantilever sheet considering different inclination angles. Qu et al. [90] optimized the experimental models analysis using a neural network analysis type NSGA II. Izamshah et al. [142] obtained a generalized force model based on ANOVA analysis, training the dataset using FEM simulations. Oliveira et al. [91] found the milling strategy (down or up milling) as the most influencing parameter for dimensional error. They also remarked that  $f_z$  had an influence on surface roughness, but only when down milling strategies were used. Borojevic et al. [92] optimized the machining time based on the machining strategy and the cutting parameters. Bolar et al. [93] and Jiang et al. [7] detected three different areas of study for roughness when flank milling of thin-wall components was performed. The first area (initial engagement) and the last one (final disengagement) are more unstable than the center of the part. Both surface and residual stresses are increased due to the forced vibrations produced by the tool on those two areas. Yan et al. [66] implemented an experimental method that allow setting the maximum depth of cut as a function of the cutting force, thus its effect does not produce any displacement on the part.

All these models can be used as simplified models to implement on adaptive control, reducing time response and modifying the cutting parameters more quickly. The effect of the cutting parameters on residual stresses, cutting forces, deflection and surface roughness is summarized in Table 2.



**Table 2.** Cutting parameters effect on residual stress, forces, deflection and roughness. S, Spindle Speed; f, feed rate; Ap, depth of cut; NP, N° of paths; MRR, Material Removal Rate; RS, Residual Stress; F, Forces; Def, Deflection; Rg, Surface Roughness.

	RS	F	Def	Rg
S	↓	↑	↑	↓
f	↑	↑	↑ / ↓ <sup>1</sup>	↑
Ap	↑	↑	↑	↑
NP	↑		↑	↑
MRR		↑		↑

<sup>1</sup> Down milling strategies increase the deflection of the part while up milling decrease it.

### 5.1.2. Virtual Twins

Another industrial approach is to develop virtual twins that will ensure the correct selection of parameters and machining strategies. Some CAM commercial software packages have optimization modules to integrate the dynamic error induced by the cutting forces as data but others only integrate the force and toolpath analysis on a FEM software. Rai et al. [5] considered elastoplastic deformation on a 3D virtual environment predicting the nonlinear behavior during machining. Jiang et al. [148] used the module VERICUT optimization to select the best parameters based on the part and tool model. This software uses neural networks to select the optimum set of parameters.

Under a set of conditions, constant thickness and cutting force, different tool paths are evaluated. Yan et al. [66] programed a depth of cut strategy simulating the physical behavior of a blade depending on the tool path generated on UG NX. The suggested variable depth of cut improves the machining error by up to 80% and save a third of the machining time. Rashev et al. [96] included artificial neural network to the CAM to improve the accuracy of the predicted deflection. Wan et al. [97] used deformation simulations to predict the optimum position of the support, evaluating the relative workpiece–part position.

Another application of virtual twins is to simulate the real position of the part. Especially mirror milling, due to their double curve, needs to use premeasuring techniques to redesign the tool-path considering the real position of the part [8,98,99]. Once it is calculated, software determines the tool path transplantation between the nominal surface and the actual one [98].

## 5.2. Adaptive Control

Adaptive control is a solution based on the on-line monitoring of the machining and an instant intervention on the process to ensure the final quality of the part. Signal data processing and monitoring systems are the base for automatic responses through parameter modification or active damping actuators. These options generally improve the vibration behavior of the system. Meanwhile, on-line measurement systems are used to reduce dimensional errors.

### 5.2.1. Monitoring

The on-line detection of vibrations, combined with SLD data and dynamic or database models, can lead to adaptive control systems able to improve final quality of the part [106]. For that, a monitoring system able to distinguish the stability or instability of the process is required. Different authors have worked to implement filters and detection systems so parameter changes can be applied.

On the vibration field, Rubeo et al. [107] used the peak-to-peak force diagrams to detect instability. Germashev et al. [40] presented a simple FFT as a tool for prediction analysis and related the fluctuation of the tool with the surface quality. Tian et al. [26] proposed a matrix perturbation method as a time saving way to obtain the natural resonance frequency in thin-wall parts while they are machined. Tian

et al. [45] used an eigenvalue sensitivity method to improve machining stability and the final surface finishing. Liu et al. [105] applied different filters to the cutting force in order to analyze the cutting coefficient behavior and its effect on the stability of the system. Liu et al. [108,109] used a Q-factor method to identify the change on the machining operation between the stable and chatter regions. The method was used for flank and mirror milling and quantified the level of chatter based on the force signal. Muhammad et al. [110] designed an active control system based on operational amplifier circuits where they can control the instant vibration, recording the acoustic signal with a microphone. Based on a dynamic model, the damping system changed the applied force so the chatter was reduced. Liu et al. [95] considered the deformation of the tool and the workpiece using an approach based on multisensor fusion and support vector machine (SVM) as a machine learning analysis. The recorded signal was analyzed using wavelet decomposition, and then SVM was applied to signal whether a change on the machining condition was needed. Ma et al. [111] developed a model to be implemented in adaptive control in which the feed rate was modified as a function of the real chip thickness. Feng et al. [32] established a different chatter model based on wavelet analysis of the cutting forces. They also studied its influence on the roughness of the part. Wan et al. [100] proposed a method for the chatter identification on thin-wall machining using a Hilbert–Huan transform and Gao et al. [101] used Complex Morlet Wavelet Transform (CMWT) to detect chatter in thin-wall machining.

Similarly, different techniques have been tested to prevent part deflection. On-line techniques have been developed based on signal treatment or on-line measurements. Wang et al. [102] used the lifting wavelet transform of the cutting forces to identify the bending of the part. Liu et al. [103] employed the cutting forces combined with a dynamic feature model that established the error compensation on real time to avoid the deformation. This solution considerably reduced the thickness error of the final part. Similarly, Han et al. [78] designed a parameter optimization federate control algorithm based on a previous simulation study of the deflection of the part that can be implemented as a control strategy schedule in an open modular architecture CNC system (OMACS). The control strategy schedule was based on the Brent–Dekker algorithm and it was successfully implemented as an adaptive control. Ma et al. [104] discovered the relationship between the induced residual stresses and the cutting power that can be used as a parameter in an on-line measuring method to avoid the deflections caused by residual stress.

### 5.2.2. Measurements

As explained above, geometrical errors can be reduced by adjusting the depth of cut as a function of the real position of the part surface. However, the instant deformation of the part caused by the machining process is difficult to predict with pre-machining analysis, especially for complex components. Following this principle, some authors have proposed measuring the position of the workpiece on-line in order to ensure its final dimension and its surface quality.

Optical techniques were tested to define the cause of the part deflection [112]. Despite experiments related to the cutting conditions with the mechanical deformation, the acquired geometrical data were not used to reduce dimensional errors.

Touching displacement sensors have also been studied for on-line measurements. Wang et al. [113] adjusted the cutting depth according to the geometrical deviations of the thin-wall, which were measured before the finishing stage on the same milling machine where the rough machining was performed. The measurements allowed calculating the depth compensation value. Similarly, Hao et al. [106] reconstructed the real in-process surface using a displacement sensor. They developed an algorithm to adjust the toolpath and the machining sequence depending on the instant deformation of the part. Their results are shown in Figure 12.

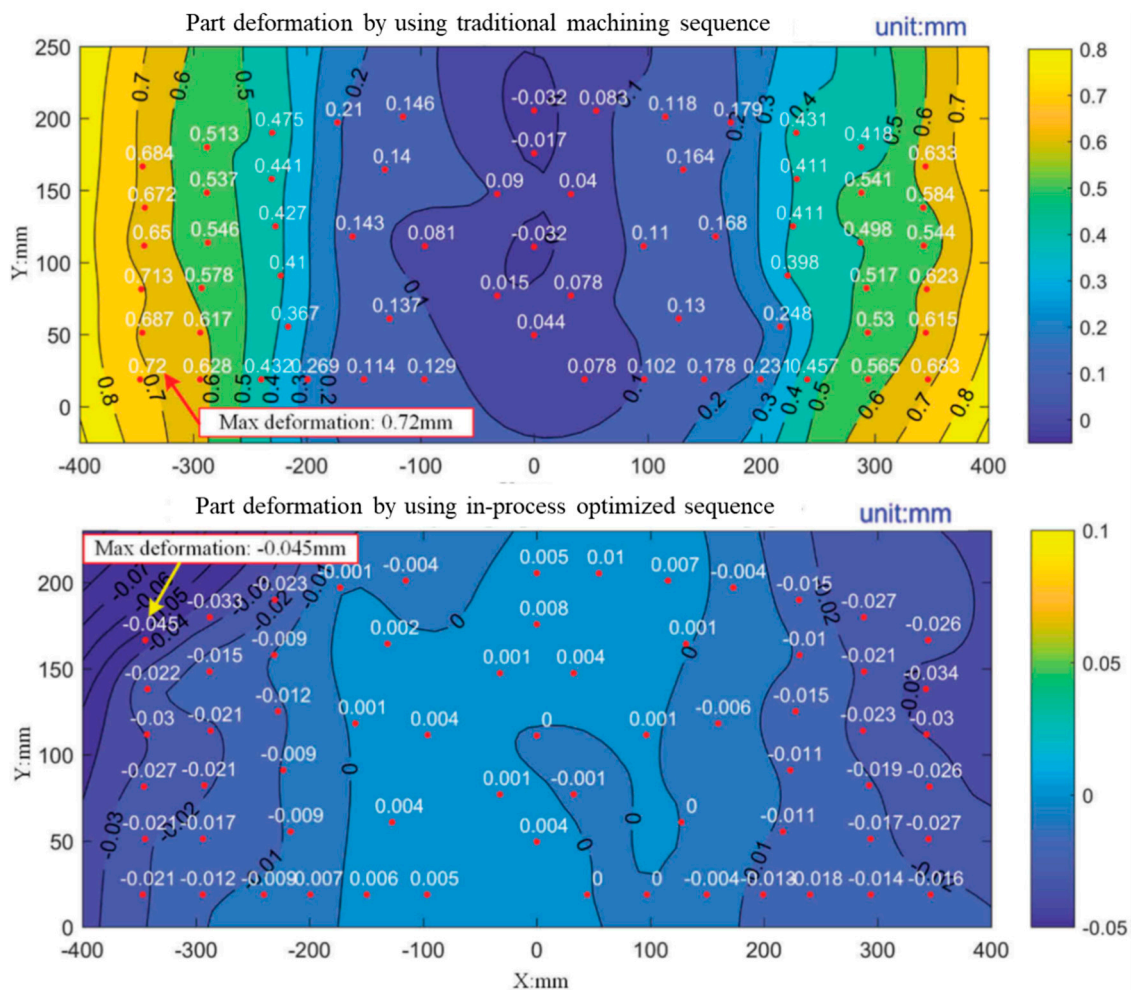


**Figure 12.** Part deformation obtained with a traditional machining sequence (upper) and with an adaptive machining system selecting an optimized sequence (lower) [106].

Other authors have tested ultrasonic devices for this purpose. Huang et al. [114] automatically recalculated the new tool position combining ultrasonic on-line measures and touching measures of a tank bottom. Rubio et al. [115] designed a flexible clamping system with an ultrasonic premeasure device that automatically adjusted the depth of cut to ensure the final thickness of the skin.

In the same way, Wang et al. [116] used a laser displacement sensor included on the supporting head to measure the in-process displacements of the workpiece. They implemented a forecasting compensatory control system to predict the skin deflection and to adaptively control the width of cut improving the quality of the final part.

### 5.3. Fixtures, Workholdings and Stiffening Devices

A different strategy to prevent instabilities during low rigidity part machining is to address this problem from the fixing perspective. This strategy could be more efficient than selecting free chatter cutting parameters for complex parts, as FRF is difficult to obtain and it is continuously changing during machining operation.

#### 5.3.1. Fixtures and Workholdings

One of the most common fixture systems for thin-wall parts are vacuum fixtures [83,116–120]. Vacuum fixture applications are based on two main two options: customized vacuum systems or flexible vacuum cups. Their use can reduce vibration and deflection [27]. On the one hand, customized



vacuum systems use special vacuum adsorption equipment for each part to be machined [120]. This option is expensive and limited to the number of equal parts produced. Moreover, the vacuum table can produce a tensile stress on the part, affecting the part deformation [12,83]. On the other hand, adaptable vacuum cups or beds increase the flexibility of the clamping fixture. This solution is based on flexible pins combined with vacuum caps or heads that adapt the position to the curves of the part [121]. Some researchers have used the virtual twin concept to select the positions of the additional supports needed for these parts [122–126]. They simulated the system obtaining a minimum part deformation. However, for large skin panels, the support provided by the cups is not enough to reduce deflection or could need a complex optimization of the cup position to reduce it [76,117]. For this reason, Rubio et al. [127] developed a flexible vacuum bed insuring the contact between the part and the workholding, reducing both vibration and deflection.

Impellers, blades and blisks are usually clamped using hydraulic chunks or special jaws that try to reduce the clamping pressure, reducing the possible in-process deformation. These systems can avoid vibrations and deflection for the initial roughing steps but machining performance can be improved using additional workholding. To increase the machining parameters and the operation efficiency, flexible workholdings have been designed for the machining of thin-wall parts. These devices apply a support on the predicted optimal position based on FEM studies [24,124]. Figure 13 shows a commercial example of the company INNOCLAMP® [128]. The workholding is specially designed to compensate the cutting energy all over the part. The position is defined using simulations, and the supports are applied at the most flexible positions. The system usually has embedded sensors, thus it is possible to change the behavior of the workholding, depending on the operation and to register historical data to feed new databases.

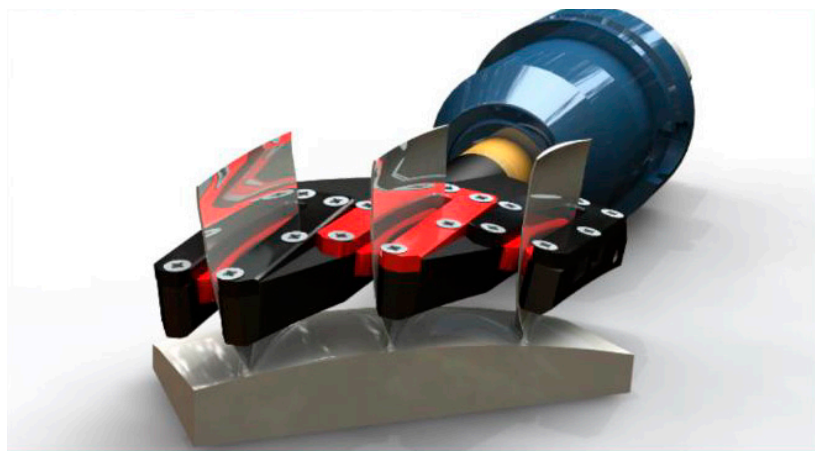


**Figure 13.** Innoclamp® holding system [128].

Alternatively, moving fixtures are used to maintain stability during low rigidity part machining. Most of the solutions are based on the mirror milling concept, a supporting element that moves synchronously to the tool. For instance, Fei et al. [48] designed a supporting element that moves collinear to the tool-path, acting as support of the cutting force. They compared the results with and without the fixing element, verifying the suppression of the deformation during the machining and the decrease of vibration amplitude, improving consequently the final roughness. Similarly, Liu et al. [129] proposed the use of an air jet to reduce deflection on the part. The jet was synchronized with the machined head following the mirror milling criteria. It impacted on one side of the wall, acting as a support of the cutting forces. Its effect was evaluated through vibration, cutting forces, thickness and final roughness data. Cutting experiments proved that the air jet assistance reduced the vibration of the workpiece up to 47% and both, thickness error and machined surface quality, were improved. However, both systems [48,129] are used for sample parts and the flexibility of it application is questionable, especially for complex geometries.

Mahmud et al. [75] tested a more sophisticated moving fixture to hold a fuselage panel, while skin panel pockets were milled. A magnetic workholding, made up of two sets of magnets, held the fuselage panel. The master set of magnets was placed on the mill tool side, following the tool trajectory provided by the milling machine. The slave set was located on the fuselage panel back and it followed the master module, compensating the cutting forces by the magnetic attraction force. It was experimentally verified that magnetic forces supported the milling thrust force and they overcame the frictional force on the slave unit.

Similar fixing systems were designed by machine tool makers such as Dufieux [130] and M. Torres [131]. They developed a mirror machine center provided with a double-head mechanism. The cutting tool installed on one head is used to remove materials from one side of the skin. Meanwhile, a twin head moves simultaneously providing an auxiliary support while the skin thickness is measured on-line to control the tool position and the depth of cut along the tool trajectory. Even though these solutions have already been implemented at industrial level for fuselage panels milling, they are still limited due to their high investment costs and need to use premeasuring techniques to redesign the tool-path considering the real position of the part.

### 5.3.2. Active Damping Actuators

Active dampers have the ability to accommodate variable conditions where they are more difficult to implement. It is a specific part of the adaptive control in which the main objective is to avoid vibrations. In this case, the adaptive control makes the decision based on the monitoring system and actuates through piezo-actuator sensors or eddy current damping (EDC). Although active damping is more difficult to implement in real industrial environments, using this approach, a sevenfold improvement in the limiting depth of cut can be obtained. For example, Zhang and Sims [132] reported workpiece chatter avoidance in milling using piezoelectric active damping mounted directly on the workpiece. The research was done on simple geometry parts such as a cantilever plate. Diez et al. [133] used this technology to compensate the deformations of the part, improving final dimensional error. Rashid and Nicolescu [134] proposed an active control of workpiece vibrations in milling through piezo-actuators embedded in workholding systems. Although the tested part had a simple geometry (rectangular blocks) and it was dynamically stiff, the vibration active control improved the dynamics of the workholding system by cancelling the vibration signal generated by the cutting process, succeeding in improving surface quality and tool life.

Yang et al. [135] designed an active and lightweight device based on EDC to attenuate the vibrations produced during the machining of a thin-walled aluminum frame. They attached an ECD to the workpiece, which vibrated synchronously to it. Based on the electromagnetic induction, when a relative motion against the magnet appears, the magnetic flux through a conductor changes and a repulsive force is generated, attenuating the vibration. ECD demonstrated the capacity of keeping the process stable under different cutting parameters ( $f_z$ ,  $S$ , and  $a_p$ ), achieving a reduction of the machining vibrations of up to 84%.

### 5.3.3. Stiffening Devices

Stiffening devices, opposite to active damping, add an extra device to the flexible component such as mass compensation system [136], magnetorheological fluids [47,137] or low melting alloys [138]. Their main advantages are the simplicity of their design and their easy implementation. However, they do not consider the stiffness change.

Trying to increase the rigidity of the part, Diaz et al. [137] investigated the use magnetorheological fluids (MRF) to prevent instabilities during thin-floor parts machining. These types of fluids have the ability to change from liquid to a semi-solid state due to the action of a magnetic field. Instead of applying variable cutting conditions to avoid chatter, they proposed the use of a shock absorber based on MRF. The way to assembly the shock absorber to the workpiece, the amount of fluid and how much voltage needed to be applied are issues of vital importance to make the shock absorber work correctly.

Experiments proved it was possible to reach optimum machining speeds in the absence of instabilities during the machining of a thin-floor part. Wang et al. [138] investigated the use of a low-melting point alloy (LMPA) as a phase change material to configure flexible fixtures. This research was focused on complex thin-walled parts, which are difficult to clamp due to the low thickness of the walls. The LMPA was heated up to 70 °C—its melting point—and casted in the gap between the part and a rigid fixture to form a rigid body with fixture among the LMPA, the fixture and the part. The LMPA increased the rigidity of the component during machining. It also reduced the deformation and the vibrations caused by the milling forces, significantly improving the machining accuracy. Furthermore, once the LMPA was melted again, almost no impact was observable on the workpiece.

Other authors have focused their studies on mass compensation systems. Kolluru et al. [139] added a viscoelastic passive dampers to minimize machining vibrations in a ring-type workpiece. A viscoelastic tape (3M® ISD112) was used to place the tuned damper blocks. The viscoelastic tape thickness, its weight and the position of the tuned mass were optimized using FEM. The dynamic response of the workpiece with and without dampers was simulated and the predicted responses were validated by impact hammer tests. The efficacy of dampers blocks was evaluated by machining undamped casing and damped casing and their use provided a significant reduction in vibration in terms of root mean square error. The author affirmed this solution can be rapidly adapted to other workpiece geometries using the FEM model they developed.

A similar approach was reported by Woody et al. [140], who addressed the potential of energy absorbing urethane foams as a passive damping to improve the dynamic behavior of an open-back. Different damping configurations were simulated and tested by FEM and experimental analysis. FRF measurements proved that the energy absorbing foam fabricated from urethane increased the damping performance by sixty times, adding less than 6% of mass compared to the overall structure. Both studies [139,140] agreed that the position of the material was important to define the clamping system, being the highest weight the most relevant factor.

Nevertheless, once a specific step of the machining process is reached, it is possible to detect a decrease on the efficiency of the damper compensating the FRF of the system. For this reason, Yang et al. [136] proposed a passive damper with tunable stiffness to suppress the wide range of vibration frequencies covered on the thin-wall machining. The ratio between the FRF of the passive damper and the workpiece varies with the material removal, especially for the thin-walled part. For this reason, they located a damper inside the workpiece and changed its orientation, modifying the workpiece stiffness. The amplitude of the workpiece FRF at the target mode was reduced by 40%, decreasing the machining vibrations and the surface roughness.

## 6. Conclusions

This work presents the state of the art of thin-wall machining. This machining usually presents dynamic and static problems that should be controlled to ensure the final quality of the part. Analytic models allow understanding the behavior of the system, defining where vibration or deflection appear. They are also the base of the computational solutions where the most significant advances have been focused on including mass loss and stiffness variation, reducing computational time and increasing prediction accuracy.

Industrial approach have been focused on the following:

- Virtual twins development integrates CAM and simulation to predict the machining behavior, the future real position of the surface to cut, and improve the machining efficiency by selecting the proper cutting parameter, toolpath, or prediction [152].
- Adaptive control, which is used in production to improve the part quality and to feed the database models, detects the process instabilities or deformation through signal analysis and changing on-line the machining parameters.

- Fixture systems design and new approaches try to include adaptive control on the workholding or the stiffening devices to increase the product efficiency, allowing to use more aggressive cutting parameters.

Overall, these studies highlight the need for more accurate simulations and control of the machining process [153]. On the one hand, there remain several aspects of computational modeling about which is little known, particularly computational time reduction is needed to consider the simulation of complex final geometries.

On the other hand, a roughness control method should be designed to detect on-line vibration and deflection with a shorter time response. For example, real-time networks could be implemented using an Internet of Things approach to collect and treat data. The improvement of interfaces and connectivity could lead to avoiding reprocessing steps. Intelligent machine control could also be achieved through machine learning or metaheuristic algorithm analysis of big data. New processing schemes can be investigated for machining time and part deformation reduction, such as simultaneous machining for monolithic parts. Considering all of this evidence, it seems that industry 4.0 outlines are not completely integrated and their integration could make thin-wall machining more profitable.

**Author Contributions:** Conceptualization, I.D.S. and A.J.G.; formal analysis, I.D.S. and A.R.; investigation, I.D.S.; writing—original draft preparation, I.D.S.; writing—review and editing, A.R., L.N.L.d.L. and A.J.G.; supervision, L.N.L.d.L. and A.R.; project administration, A.J.G.; and funding acquisition, L.N.L.d.L.

**Funding:** This research was funded by University of Cadiz, UCA/REC01VI/2016.

**Acknowledgments:** Figure 9 reprinted by permission from RightsLink Permissions: (Springer) (The International Journal of Advanced Manufacturing Technology) (Finite strip modeling of the varying dynamics of thin-walled pocket structures during machining, Keivan Ahmadi), (2016). Figure 10 reprinted by permission from RightsLink Permissions: (Springer) (The International Journal of Advanced Manufacturing Technology) (Cutting deflection control of the blade based on real-time feedrate scheduling in open modular architecture CNC system, Zhenyu Han, Hongyu Jin, Yunzhong Fu et al.), (2016). Figure 11 reprinted by permission of the publisher (Taylor & Francis Ltd., <http://www.tandfonline.com>) from Dynamic machining process planning incorporating in-process workpiece deformation data for large-size aircraft structural parts, Xiaozhong Hao, Yingguang Li, et al., International Journal of Computer Integrated Manufacturing, 2019.

**Conflicts of Interest:** The authors declare no conflict of interest.

## References

1. Herranz, S.; Campa, F.J.; López de Lacalle, L.N.; Rivero, A.; Lamikiz, A.; Ukar, E.; Sánchez, J.A.; Bravo, U. The milling of airframe components with low rigidity: A general approach to avoid static and dynamic problems. *Proc. Inst. Mech. Eng. Part B J. Eng. Manuf.* **2005**, *219*, 789–801. [[CrossRef](#)]
2. Li, X.; Zhao, W.; Li, L.; He, N.; Chi, S. Modeling and application of process damping in milling of thin-walled workpiece made of titanium alloy. *Shock Vib.* **2015**, *2015*. [[CrossRef](#)]
3. Bravo, U.; Altuzarra, O.; López de Lacalle, L.N.; Sánchez, J.A.A.; Campa, F.J.J. Stability limits of milling considering the flexibility of the workpiece and the machine. *Int. J. Mach. Tools Manuf.* **2005**, *45*, 1669–1680. [[CrossRef](#)]
4. Arnaud, L.; Gonzalo, O.; Seguy, S.; Jauregi, H.; Peigné, G. Simulation of low rigidity part machining applied to thin-walled structures. *Int. J. Adv. Manuf. Technol.* **2010**, *54*, 479–488. [[CrossRef](#)]
5. Rai, J.K.; Xirouchakis, P. Finite element method based machining simulation environment for analyzing part errors induced during milling of thin-walled components. *Int. J. Mach. Tools Manuf.* **2008**, *48*, 629–643. [[CrossRef](#)]
6. Chen, W.; Xue, J.; Tang, D.; Chen, H.; Qu, S. Deformation prediction and error compensation in multilayer milling processes for thin-walled parts. *Int. J. Mach. Tools Manuf.* **2009**, *49*, 859–864. [[CrossRef](#)]
7. Jiang, X.; Zhu, Y.; Zhang, Z.; Guo, M.; Ding, Z. Investigation of residual impact stress and its effects on the precision during milling of the thin-walled part. *Int. J. Adv. Manuf. Technol.* **2018**, *97*, 877–892. [[CrossRef](#)]
8. Bi, Q.; Huang, N.; Zhang, S.; Shuai, C.; Wang, Y. Adaptive machining for curved contour on deformed large skin based on on-machine measurement and isometric mapping. *Int. J. Mach. Tools Manuf.* **2019**, *136*, 34–44. [[CrossRef](#)]

9. Amended WP & Budget 4th Call for Proposals (CFP04): Preliminary List and Full Description of Topics; European Union Funding for Research & Innovation: Brussel, Belgium, 2016; p. 219.
10. Tang, A.; Liu, Z. Three-dimensional stability lobe and maximum material removal rate in end milling of thin-walled plate. *Int. J. Adv. Manuf. Technol.* **2009**, *43*, 33–39. [[CrossRef](#)]
11. Ratchev, S.; Liu, S.; Huang, W.; Becker, A.A. A flexible force model for end milling of low-rigidity parts. *J. Mater. Process. Technol.* **2004**, *153–154*, 134–138. [[CrossRef](#)]
12. Richter-Trummer, V.; Koch, D.; Witte, A.; Dos Santos, J.F.; De Castro, P.M.S.T. Methodology for prediction of distortion of workpieces manufactured by high speed machining based on an accurate through-the-thickness residual stress determination. *Int. J. Adv. Manuf. Technol.* **2013**, *68*, 2271–2281. [[CrossRef](#)]
13. Izamshah, R.A. *Hybrid Deflection Prediction for Machining Thin-Wall Titanium Alloy Aerospace Component*; RMIT: Melbourne, Australia, 2011.
14. Biermann, D.; Kersting, P.; Surmann, T. A general approach to simulating workpiece vibrations during five-axis milling of turbine blades. *CIRP Ann. Manuf. Technol.* **2010**, *59*, 125–128. [[CrossRef](#)]
15. Yan, R.; Gong, Y.; Peng, F.; Tang, X.; Li, H.; Li, B. Three degrees of freedom stability analysis in the milling with bull-nosed end mills. *Int. J. Adv. Manuf. Technol.* **2016**, *86*, 71–85. [[CrossRef](#)]
16. Guo, Q.; Jiang, Y.; Zhao, B.; Ming, P. Chatter modeling and stability lobes predicting for non-uniform helix tools. *Int. J. Adv. Manuf. Technol.* **2016**, *87*, 251–266. [[CrossRef](#)]
17. Kolluru, K.V.; Axinte, D.; Becker, A. A solution for minimising vibrations in milling of thin walled casings by applying dampers to workpiece surface. *CIRP Ann. Manuf. Technol.* **2013**, *62*, 415–418. [[CrossRef](#)]
18. Feng, J.; Wan, M.; Gao, T.Q.; Zhang, W.H. Mechanism of process damping in milling of thin-walled workpiece. *Int. J. Mach. Tools Manuf.* **2018**, *134*, 1–19. [[CrossRef](#)]
19. Ding, Y.; Zhu, L. Investigation on chatter stability of thin-walled parts considering its flexibility based on finite element analysis. *Int. J. Adv. Manuf. Technol.* **2018**, *94*, 3173–3187. [[CrossRef](#)]
20. Fei, J.; Lin, B.; Yan, S.; Zhang, X.; Lan, J.; Dai, S. Chatter prediction for milling of flexible pocket-structure. *Int. J. Adv. Manuf. Technol.* **2017**, *89*, 2721–2730. [[CrossRef](#)]
21. Yang, Y.; Zhang, W.H.; Ma, Y.C.; Wan, M. Chatter prediction for the peripheral milling of thin-walled workpieces with curved surfaces. *Int. J. Mach. Tools Manuf.* **2016**, *109*, 36–48. [[CrossRef](#)]
22. Budak, E. Mechanics and Dynamics of Milling Thin Walled Structures. Ph.D. Thesis, University of British Columbia, Vancouver, BC, Canada, 1994. [[CrossRef](#)]
23. Budak, E.; Altintas, Y.; Armarego, E.J.A. Prediction of Milling Force Coefficients from Orthogonal Cutting Data. *J. Manuf. Sci. Eng.* **1996**, *118*, 216. [[CrossRef](#)]
24. Wang, H.; Huang, L.; Yao, C.; Kou, M.; Wang, W.; Huang, B.; Zheng, W. Integrated analysis method of thin-walled turbine blade precise machining. *Int. J. Precis. Eng. Manuf.* **2015**, *16*, 1011–1019. [[CrossRef](#)]
25. Qu, S.; Zhao, J.; Wang, T. Three-dimensional stability prediction and chatter analysis in milling of thin-walled plate. *Int. J. Adv. Manuf. Technol.* **2016**, *86*, 2291–2300. [[CrossRef](#)]
26. Tian, W.; Ren, J.; Zhou, J.; Wang, D. Dynamic modal prediction and experimental study of thin-walled workpiece removal based on perturbation method. *Int. J. Adv. Manuf. Technol.* **2018**, *94*, 2099–2113. [[CrossRef](#)]
27. Campa, F.J.; López de Lacalle, L.N.; Celaya, A. Chatter avoidance in the milling of thin floors with bull-nose end mills: Model and stability diagrams. *Int. J. Mach. Tools Manuf.* **2011**, *51*, 43–53. [[CrossRef](#)]
28. Zhang, J.; Lin, B.; Fei, J.; Huang, T.; Xiao, J.; Zhang, X.; Ji, C. Modeling and experimental validation for surface error caused by axial cutting force in end-milling process. *Int. J. Adv. Manuf. Technol.* **2018**, *99*, 327–335. [[CrossRef](#)]
29. Yang, Y.; Zhang, W.-H.; Ma, Y.-C.; Wan, M.; Dang, X.-B. An efficient decomposition-condensation method for chatter prediction in milling large-scale thin-walled structures. *Mech. Syst. Signal. Process.* **2019**, *121*, 58–76. [[CrossRef](#)]
30. Jin, X.; Sun, Y.; Guo, Q.; Guo, D. 3D stability lobe considering the helix angle effect in thin-wall milling. *Int. J. Adv. Manuf. Technol.* **2016**, *82*, 2123–2136. [[CrossRef](#)]
31. Li, Z.; Sun, Y.; Guo, D. Chatter prediction utilizing stability lobes with process damping in finish milling of titanium alloy thin-walled workpiece. *Int. J. Adv. Manuf. Technol.* **2017**, *89*, 2663–2674. [[CrossRef](#)]
32. Feng, J.; Sun, Z.; Jiang, Z.; Yang, L. Identification of chatter in milling of Ti-6Al-4V titanium alloy thin-walled workpieces based on cutting force signals and surface topography. *Int. J. Adv. Manuf. Technol.* **2016**, *82*, 1909–1920. [[CrossRef](#)]



33. Budak, E.; Tunç, L.T.; Alan, S.; Özgüven, H.N. Prediction of workpiece dynamics and its effects on chatter stability in milling. *CIRP Ann.* **2012**, *61*, 339–342. [[CrossRef](#)]
34. Wu, Q.; Li, D.-P.; Ren, L.; Mo, S. Detecting milling deformation in 7075 aluminum alloy thin-walled plates using finite difference method. *Int. J. Adv. Manuf. Technol.* **2016**, *85*, 1291–1302. [[CrossRef](#)]
35. Han, D.; Li, P.; An, S.; Shi, P. Multi-frequency weak signal detection based on wavelet transform and parameter compensation band-pass multi-stable stochastic resonance. *Mech. Syst. Signal. Process.* **2016**, *71–71*, 995–1010. [[CrossRef](#)]
36. Scippa, A.; Grossi, N.; Campatelli, G. FEM based cutting velocity selection for thin walled part machining. *Procedia CIRP* **2014**, *14*, 287–292. [[CrossRef](#)]
37. Campa, F.J.; López de Lacalle, L.N.; Lamikiz, A.; Sánchez, J.A. Selection of cutting conditions for a stable milling of flexible parts with bull-nose end mills. *J. Mater. Process. Technol.* **2007**, *191*, 279–282. [[CrossRef](#)]
38. Bolsunovskiy, S.; Vermel, V.; Gubanov, G.; Kacharava, I.; Kudryashov, A. Thin-Walled Part Machining Process Parameters Optimization based on Finite-Element Modeling of Workpiece Vibrations. *Procedia CIRP* **2013**, *8*, 276–280. [[CrossRef](#)]
39. Olvera, D.; Urbikain, G.; Elías-Zuñiga, A.; López de Lacalle, L. Improving Stability Prediction in Peripheral Milling of Al7075T6. *Appl. Sci.* **2018**, *8*, 1316. [[CrossRef](#)]
40. Germashev, A.; Logominov, V.; Anpilogov, D.; Vnukov, Y.; Khristal, V. Optimal cutting condition determination for milling thin-walled details. *Adv. Manuf.* **2018**, *6*, 280–290. [[CrossRef](#)]
41. Urbikain Pelayo, G.; López De La Calle, L. Stability charts with large curve-flute end-mills for thin-walled workpieces. *Mach. Sci. Technol.* **2018**, *22*, 585–603. [[CrossRef](#)]
42. Yan, Z.; Liu, Z.; Wang, X.; Liu, B.; Luo, Z.; Wang, D. Stability prediction of thin-walled workpiece made of Al7075 in milling based on shifted Chebyshev polynomials. *Int. J. Adv. Manuf. Technol.* **2016**, *87*, 115–124. [[CrossRef](#)]
43. Urbikain, G.; Artetxe, E.; López de Lacalle, L.N. Numerical simulation of milling forces with barrel-shaped tools considering runout and tool inclination angles. *Appl. Math. Model.* **2017**, *47*, 619–636. [[CrossRef](#)]
44. Ma, J.; Zhang, D.; Liu, Y.; Wu, B.; Luo, M. Tool posture dependent chatter suppression in five-axis milling of thin-walled workpiece with ball-end cutter. *Int. J. Adv. Manuf. Technol.* **2017**, *91*, 287–299. [[CrossRef](#)]
45. Tian, W.; Ren, J.; Wang, D.; Zhang, B. Optimization of non-uniform allowance process of thin-walled parts based on eigenvalue sensitivity. *Int. J. Adv. Manuf. Technol.* **2018**, *96*, 2101–2116. [[CrossRef](#)]
46. Xu, C.; Feng, P.; Zhang, J.; Yu, D.; Wu, Z. Milling stability prediction for flexible workpiece using dynamics of coupled machining system. *Int. J. Adv. Manuf. Technol.* **2017**, *90*, 3217–3227. [[CrossRef](#)]
47. Ma, J.; Zhang, D.; Wu, B.; Luo, M.; Chen, B. Vibration suppression of thin-walled workpiece machining considering external damping properties based on magnetorheological fluids flexible fixture. *Chin. J. Aeronaut.* **2016**, *29*, 1074–1083. [[CrossRef](#)]
48. Fei, J.; Lin, B.; Xiao, J.; Ding, M.; Yan, S.; Zhang, X.; Zhang, J. Investigation of moving fixture on deformation suppression during milling process of thin-walled structures. *J. Manuf. Process.* **2018**, *32*, 403–411. [[CrossRef](#)]
49. Wang, L.; Si, H. Machining deformation prediction of thin-walled workpieces in five-axis flank milling. *Int. J. Adv. Manuf. Technol.* **2018**, *97*, 4179–4193. [[CrossRef](#)]
50. Song, Q.; Liu, Z.; Wan, Y.; Ju, G.; Shi, J. Application of Sherman-Morrison-Woodbury formulas in instantaneous dynamic of peripheral milling for thin-walled component. *Int. J. Mech. Sci.* **2015**, *96–97*, 79–90. [[CrossRef](#)]
51. Ding, H.; Ke, Y. Study on Machining Deformation of Aircraft Monolithic Component by FEM and Experiment. *Chin. J. Aeronaut.* **2006**, *19*, 247–254. [[CrossRef](#)]
52. Gradišek, J.; Kalveram, M.; Weinert, K. Mechanistic identification of specific force coefficients for a general end mill. *Int. J. Mach. Tools Manuf.* **2004**, *44*, 401–414. [[CrossRef](#)]
53. Kang, Y.-G.; Wang, Z.-Q. Two efficient iterative algorithms for error prediction in peripheral milling of thin-walled workpieces considering the in-cutting chip. *Int. J. Mach. Tools Manuf.* **2013**, *73*, 55–61. [[CrossRef](#)]
54. Barbero, B.R.; Ureta, E.S. Comparative study of different digitization techniques and their accuracy. *CAD Comput. Aided Des.* **2011**, *43*, 188–206. [[CrossRef](#)]
55. Ahmadi, K. Finite strip modeling of the varying dynamics of thin-walled pocket structures during machining. *Int. J. Adv. Manuf. Technol.* **2017**, *89*, 2691–2699. [[CrossRef](#)]
56. Lin, X.; Wu, D.; Yang, B.; Wu, G.; Shan, X.; Xiao, Q.; Hu, L.; Yu, J. Research on the mechanism of milling surface waviness formation in thin-walled blades. *Int. J. Adv. Manuf. Technol.* **2017**, *93*, 2459–2470. [[CrossRef](#)]

57. Tuysuz, O.; Altintas, Y. Frequency Domain Updating of Thin-Walled Workpiece Dynamics Using Reduced Order Substructuring Method in Machining. *J. Manuf. Sci. Eng.* **2017**, *139*, 071013. [[CrossRef](#)]
58. Ratchev, S.; Liu, S.; Becker, A.A.A. Error compensation strategy in milling flexible thin-wall parts. *J. Mater. Process. Technol.* **2005**, *162–163*, 673–681. [[CrossRef](#)]
59. Shuang, F.; Chen, X.; Ma, W. Numerical analysis of chip formation mechanisms in orthogonal cutting of Ti6Al4V alloy based on a CEL model. *Int. J. Mater.* **2018**, *11*, 185–198. [[CrossRef](#)]
60. Elbestawi, M.A.; Sagherian, R. Dynamic modeling for the prediction of surface errors in the milling of thin-walled sections. *J. Mater. Process. Technol.* **1991**, *25*, 215–228. [[CrossRef](#)]
61. Tsai, J.-S.; Liao, C.-L. Finite-element modeling of static surface errors in the peripheral milling of thin-walled workpieces. *J. Mater. Process. Technol.* **1999**, *94*, 235–246. [[CrossRef](#)]
62. Ratchev, S.; Govender, E.; Nikov, S.; Phuah, K.; Tsiklos, G. Force and deflection modelling in milling of low-rigidity complex parts. *J. Mater. Process. Technol.* **2003**, *143–144*, 796–801. [[CrossRef](#)]
63. Wan, M.; Zhang, W.H.; Qin, G.H.; Wang, Z.P. Strategies for error prediction and error control in peripheral milling of thin-walled workpiece. *Int. J. Mach. Tools Manuf.* **2008**, *48*, 1366–1374. [[CrossRef](#)]
64. Li, M.; Huang, J.; Ding, W.; Liu, X.; Li, L. Dynamic response analysis of a ball-end milling cutter and optimization of the machining parameters for a ruled surface. *Proc. Inst. Mech. Eng. Part B J. Eng. Manuf.* **2019**, *233*, 588–599. [[CrossRef](#)]
65. Jiang, X.; Wang, Y.; Ding, Z.; Li, H. An approach to predict the distortion of thin-walled parts affected by residual stress during the milling process. *Int. J. Adv. Manuf. Technol.* **2017**, *93*, 4203–4216. [[CrossRef](#)]
66. Yan, Q.; Luo, M.; Tang, K. Multi-axis variable depth-of-cut machining of thin-walled workpieces based on the workpiece deflection constraint. *CAD Comput. Aided Des.* **2018**, *100*, 14–29. [[CrossRef](#)]
67. Aijun, T.; Zhanqiang, L. Deformations of thin-walled plate due to static end milling force. *J. Mater. Process. Technol.* **2008**, *206*, 345–351. [[CrossRef](#)]
68. Wan, M.; Zhang, W.H. Calculations of chip thickness and cutting forces in flexible end milling. *Int. J. Adv. Manuf. Technol.* **2006**, *29*, 637–647. [[CrossRef](#)]
69. Du, Z.; Zhang, D.; Hou, H.; Liang, S.Y. Peripheral milling force induced error compensation using analytical force model and APDL deformation calculation. *Int. J. Adv. Manuf. Technol.* **2017**, *88*, 3405–3417. [[CrossRef](#)]
70. Wang, L.; Huang, H.; West, R.W.; Li, H.; Du, J. A model of deformation of thin-wall surface parts during milling machining process. *J. Cent. South. Univ.* **2018**, *25*, 1107–1115. [[CrossRef](#)]
71. Ma, J.W.; Liu, Z.; Jia, Z.Y.; Song, D.N.; Gao, Y.Y.; Si, L.K. Stability recognition for high-speed milling of TC4 thin-walled parts with curved surface. *Int. J. Adv. Manuf. Technol.* **2017**, *91*, 1–11. [[CrossRef](#)]
72. Liu, S.M.; Shao, X.D.; Ge, X.B.; Wang, D. Simulation of the deformation caused by the machining cutting force on thin-walled deep cavity parts. *Int. J. Adv. Manuf. Technol.* **2017**, *92*, 3503–3517. [[CrossRef](#)]
73. Ning, H.; Zhigang, W.; Chengyu, J.; Bing, Z. Finite element method analysis and control stratagem for machining deformation of thin-walled components. *J. Mater. Process. Technol.* **2003**, *139*, 332–336. [[CrossRef](#)]
74. Gang, L. Study on deformation of titanium thin-walled part in milling process. *J. Mater. Process. Technol.* **2009**, *209*, 2788–2793. [[CrossRef](#)]
75. Mahmud, A.; Mayer, J.R.R.; Baron, L. Magnetic attraction forces between permanent magnet group arrays in a mobile magnetic clamp for pocket machining. *CIRP J. Manuf. Sci. Technol.* **2015**, *11*, 82–88. [[CrossRef](#)]
76. Do, M.D.; Son, Y.; Choi, H.J. Optimal workpiece positioning in flexible fixtures for thin-walled components. *CAD Comput. Aided Des.* **2018**, *95*, 14–23. [[CrossRef](#)]
77. Wu, Q.; Li, D.-P. Analysis and X-ray measurements of cutting residual stresses in 7075 aluminum alloy in high speed machining. *Int. J. Precis. Eng. Manuf.* **2014**, *15*, 1499–1506. [[CrossRef](#)]
78. Han, Z.; Jin, H.; Fu, Y.; Fu, H. Cutting deflection control of the blade based on real-time feedrate scheduling in open modular architecture CNC system. *Int. J. Adv. Manuf. Technol.* **2017**, *90*, 2567–2579. [[CrossRef](#)]
79. Li, B.; Jiang, X.; Yang, J.; Liang, S.Y. Effects of depth of cut on the redistribution of residual stress and distortion during the milling of thin-walled part. *J. Mater. Process. Technol.* **2015**, *216*, 223–233. [[CrossRef](#)]
80. Ma, Y.; Liu, S.; Feng, P.F.; Yu, D.W. Finite element analysis of residual stresses and thin plate distortion after face milling. In Proceedings of the 2015 12th International Bhurban Conference on Applied Sciences and Technology (IBCAST), Islamabad, Pakistan, 13–17 January 2015; pp. 67–71. [[CrossRef](#)]
81. Jiang, X.; Li, B.; Yang, J.; Zuo, X.Y.; Li, K. An approach for analyzing and controlling residual stress generation during high-speed circular milling. *Int. J. Adv. Manuf. Technol.* **2013**, *66*, 1439–1448. [[CrossRef](#)]

82. Jiang, X.; Li, B.; Yang, J.; Zuo, X.Y. Effects of tool diameters on the residual stress and distortion induced by milling of thin-walled part. *Int. J. Adv. Manuf. Technol.* **2013**, *68*, 175–186. [[CrossRef](#)]
83. Chatelain, J.-F.; Lalonde, J.-F.; Tahan, A.S. Effect of Residual Stresses Embedded within workpieces on the distortion of parts after machining. *Int. J. Mech.* **2012**, *6*, 43–51.
84. Masoudi, S.; Amini, S.; Saeidi, E.; Eslami-Chalander, H. Effect of machining-induced residual stress on the distortion of thin-walled parts. *Int. J. Adv. Manuf. Technol.* **2014**, *76*, 597–608. [[CrossRef](#)]
85. Arrazola, P.J.; Özel, T.; Umbrello, D.; Davies, M.; Jawahir, I.S. Recent advances in modelling of metal machining processes. *CIRP Ann. Manuf. Technol.* **2013**, *62*, 695–718. [[CrossRef](#)]
86. Gao, H.; Zhang, Y.; Wu, Q.; Li, B. Investigation on influences of initial residual stress on thin-walled part machining deformation based on a semi-analytical model. *J. Mater. Process. Technol.* **2018**, *262*, 437–448. [[CrossRef](#)]
87. Hao, Y.; Liu, Y. Analysis of milling surface roughness prediction for thin-walled parts with curved surface. *Int. J. Adv. Manuf. Technol.* **2017**, *93*, 2289–2297. [[CrossRef](#)]
88. Wu, Q.; Li, D.-P.; Zhang, Y.-D. Detecting Milling Deformation in 7075 Aluminum Alloy Aeronautical Monolithic Components Using the Quasi-Symmetric Machining Method. *MET Archit.* **2016**, *6*, 80. [[CrossRef](#)]
89. Sonawane, H.A.; Joshi, S.S. Modeling of machined surface quality in high-speed ball-end milling of Inconel-718 thin cantilevers. *Int. J. Adv. Manuf. Technol.* **2015**, *78*, 1751–1768. [[CrossRef](#)]
90. Qu, S.; Zhao, J.; Wang, T. Experimental study and machining parameter optimization in milling thin-walled plates based on NSGA-II. *Int. J. Adv. Manuf. Technol.* **2017**, *89*, 2399–2409. [[CrossRef](#)]
91. de Oliveira, E.L.; de Souza, A.F.; Diniz, A.E. Evaluating the influences of the cutting parameters on the surface roughness and form errors in 4-axis milling of thin-walled free-form parts of AISI H13 steel. *J. Braz. Soc. Mech. Sci. Eng.* **2018**, *40*, 334. [[CrossRef](#)]
92. Borojević, S.; Lukić, D.; Milošević, M.; Vukman, J.; Kramar, D. Optimization of process parameters for machining of Al 7075 thin—Walled structures. *Adv. Prod. Manag.* **2018**, *13*, 125–135. [[CrossRef](#)]
93. Bolar, G.; Das, A.; Joshi, S.N. Measurement and analysis of cutting force and product surface quality during end-milling of thin-wall components. *Meas. J. Int. Meas. Confed.* **2018**, *121*, 190–204. [[CrossRef](#)]
94. Del Sol, I.; Rivero, A.; Salguero, J.; Fernández-Vidal, S.R.; Marcos, M. Tool-path effect on the geometric deviations in the machining of UNS A92024 aeronautic skins. *Procedia Manuf.* **2017**, *13*, 639–646. [[CrossRef](#)]
95. Liu, C.; Li, Y.; Zhou, G.; Shen, W. A sensor fusion and support vector machine based approach for recognition of complex machining conditions. *J. Intell. Manuf.* **2018**, *29*, 1739–1752. [[CrossRef](#)]
96. Ratchev, S.; Govender, E.; Nikov, S. Towards deflection prediction and compensation in machining of low-rigidity parts. *Proc. Inst. Mech. Eng. Part B J. Eng. Manuf.* **2002**, *216*, 129–134. [[CrossRef](#)]
97. Wan, X.-J.; Hua, L.; Wang, X.-F.; Peng, Q.-Z.; Qin, X. An error control approach to tool path adjustment conforming to the deformation of thin-walled workpiece. *Int. J. Mach. Tools Manuf.* **2011**, *51*, 221–229. [[CrossRef](#)]
98. Hao, X.; Li, Y.; Deng, T.; Liu, C.; Xiang, B. Tool path transplantation method for adaptive machining of large-sized and thin-walled free form surface parts based on error distribution. *Robot. Comput. Integr. Manuf.* **2019**, *56*, 222–232. [[CrossRef](#)]
99. Wang, Y.; Hou, B.; Wang, F.; Ji, Z.; Liang, Z. Research on a thin-walled part manufacturing method based on information-localizing technology. *Proc. Inst. Mech. Eng. Part C J. Mech. Eng. Sci.* **2017**, *231*, 4099–4109. [[CrossRef](#)]
100. Wan, S.; Li, X.; Chen, W.; Hong, J. Investigation on milling chatter identification at early stage with variance ratio and Hilbert–Huang transform. *Int. J. Adv. Manuf. Technol.* **2018**, *95*, 3563–3573. [[CrossRef](#)]
101. Gao, J.; Song, Q.; Liu, Z. Chatter detection and stability region acquisition in thin-walled workpiece milling based on CMWT. *Int. J. Adv. Manuf. Technol.* **2018**, *98*, 699–713. [[CrossRef](#)]
102. Wang, G.; Yang, X.; Wang, Z. On-line deformation monitoring of thin-walled parts based on least square fitting method and lifting wavelet transform. *Int. J. Adv. Manuf. Technol.* **2018**, *94*, 4237–4246. [[CrossRef](#)]
103. Liu, C.; Li, Y.; Shen, W. A real time machining error compensation method based on dynamic features for cutting force induced elastic deformation in flank milling. *Mach. Sci. Technol.* **2018**, *22*, 766–786. [[CrossRef](#)]
104. Ma, Y.; Feng, P.; Zhang, J.; Wu, Z.; Yu, D. Energy criteria for machining-induced residual stresses in face milling and their relation with cutting power. *Int. J. Adv. Manuf. Technol.* **2015**, *81*, 1023–1032. [[CrossRef](#)]
105. Liu, X.; Gao, H.; Yue, C.; Li, R.; Jiang, N.; Yang, L. Investigation of the milling stability based on modified variable cutting force coefficients. *Int. J. Adv. Manuf. Technol.* **2018**, *96*, 2991–3002. [[CrossRef](#)]



106. Hao, X.; Li, Y.; Zhao, Z.; Liu, C. Dynamic machining process planning incorporating in-process workpiece deformation data for large-size aircraft structural parts. *Int. J. Comput. Integr. Manuf.* **2019**, *32*, 136–147. [CrossRef]
107. Rubeo, M.A.; Schmitz, T.L. Global stability predictions for flexible workpiece milling using time domain simulation. *J. Manuf. Syst.* **2016**, *40*, 8–14. [CrossRef]
108. Liu, H.; Bo, Q.; Zhang, H.; Wang, Y. Analysis of Q-factor's identification ability for thin-walled part flank and mirror milling chatter. *Int. J. Adv. Manuf. Technol.* **2018**, *99*, 1673–1686. [CrossRef]
109. Wang, Y.; Bo, Q.; Liu, H.; Hu, L.; Zhang, H. Mirror milling chatter identification using Q-factor and SVM. *Int. J. Adv. Manuf. Technol.* **2018**, *98*, 1163–1177. [CrossRef]
110. Muhammad, B.B.; Wan, M.; Liu, Y.; Yuan, H. Active Damping of Milling Vibration Using Operational Amplifier Circuit. *Chin. J. Mech. Eng.* **2018**, *31*, 90. [CrossRef]
111. Ma, J.W.; He, G.Z.; Liu, Z.; Qin, F.Z.; Chen, S.Y.; Zhao, X.X. Instantaneous cutting-amount planning for machining deformation homogenization based on position-dependent rigidity of thin-walled surface parts. *J. Manuf. Process.* **2018**, *34*, 401–411. [CrossRef]
112. Loehe, J.; Zaeh, M.F.; Roesch, O. In-Process Deformation Measurement of Thin-walled Workpieces. *Procedia CIRP* **2012**, *1*, 546–551. [CrossRef]
113. Wang, G.; Li, W.; Tong, G.; Pang, C. Improving the machining accuracy of thin-walled parts by online measuring and allowance compensation. *Int. J. Adv. Manuf. Technol.* **2017**, *92*, 2755–2763. [CrossRef]
114. Huang, N.; Yin, C.; Liang, L.; Hu, J.; Wu, S. Error compensation for machining of large thin-walled part with sculptured surface based on on-machine measurement. *Int. J. Adv. Manuf. Technol.* **2018**, *96*, 4345–4352. [CrossRef]
115. Rubio, A.; Rivero, A.; Del Sol, I.; Ukar, E.; Lamikiz, A. Capacitation of flexibles fixtures for its use in high quality machining processes: An application case of the industry 4.0 paradigm. *Dyna* **2018**, *93*, 608–612.
116. Wang, X.; Bi, Q.; Zhu, L.; Ding, H. Improved forecasting compensatory control to guarantee the remaining wall thickness for pocket milling of a large thin-walled part. *Int. J. Adv. Manuf. Technol.* **2018**, *94*, 1677–1688. [CrossRef]
117. Junbai, L.; Kai, Z. Multi-point location theory, method, and application for flexible tooling system in aircraft manufacturing. *Int. J. Adv. Manuf. Technol.* **2010**, *54*, 729–736. [CrossRef]
118. Hao, M.; Xu, D.; Wei, F.; Li, Q. Quantitative analysis of frictional behavior of cupronickel B10 at the tool-chip interface during dry cutting. *Tribol. Int.* **2018**, *118*, 163–169. [CrossRef]
119. Zhou, G.; Li, Y.; Liu, C.; Hao, X. A feature-based automatic broken surfaces fitting method for complex aircraft skin parts. *Int. J. Adv. Manuf. Technol.* **2016**, *84*, 1001–1011. [CrossRef]
120. Zhou, Z.; Zhang, H.; Xu, M. Research on precision and greenhouse manufacturing technology for large aircraft panels. *Procedia CIRP* **2016**, *56*, 565–568. [CrossRef]
121. Bumgarner, K.; Lebakken, C.; Vando, C.; Reddie, W.; Jacovetti, G. Universal Holding Fixture. U.S. Patent No. 4,684,113, 3 December 2009.
122. Zeng, S.; Wan, X.; Li, W.; Yin, Z.; Xiong, Y. A novel approach to fixture design on suppressing machining vibration of flexible workpiece. *Int. J. Mach. Tools Manuf.* **2012**, *58*, 29–43. [CrossRef]
123. Nee, A.Y.C.; Kurnar, A.S.; Tao, Z.J. An intelligent fixture with a dynamic clamping scheme. *Proc. Inst. Mech. Eng. Part B J. Eng. Manuf.* **2000**, *214*, 183–196. [CrossRef]
124. Wan, X.-J.; Zhang, Y.; Huang, X.-D. Investigation of influence of fixture layout on dynamic response of thin-wall multi-framed work-piece in machining. *Int. J. Mach. Tools Manuf.* **2013**, *75*, 87–99. [CrossRef]
125. Liu, S.G.; Jin, Q.; Wang, P. Effect of additional supports on surface errors in the peripheral milling of a flexible workpiece. *Int. J. Mater. Prod. Technol.* **2008**, *31*, 214–223. [CrossRef]
126. Liu, S.; Zheng, L.; Zhang, Z.H.; Wen, D.H. Optimal fixture design in peripheral milling of thin-walled workpiece. *Int. J. Adv. Manuf. Technol.* **2006**, *28*, 653–658. [CrossRef]
127. Rubio, A.; Calleja, L.; Orive, J.; Mújica, Á.; Rivero, A. Flexible Machining System for an Efficient Skin Machining. *SAE Tech.* **2016**, *1*, 2129. [CrossRef]
128. Innoclamp GmbH Innoclamp. Available online: <http://www.innoclamp.de/> (accessed on 6 May 2019).
129. Liu, C.; Sun, J.; Li, Y.; Li, J. Investigation on the milling performance of titanium alloy thin-walled part with air jet assistance. *Int. J. Adv. Manuf. Technol.* **2018**, *95*, 2865–2874. [CrossRef]
130. Dufieux Dufieux Industrie—Modular. Available online: <http://www.dufieux-industrie.com/en/mirror-milling-system-mms> (accessed on 2 June 2016).

131. Mtorres Surface Milling Machining. Available online: <http://www.mtorres.es/en/aeronautics/products/metallic/torres-surface-milling> (accessed on 2 June 2016).
132. Zhang, Y.M.; Sims, N.D. Milling workpiece chatter avoidance using piezoelectric active damping: A feasibility study. *Smart Mater. Struct.* **2005**, *14*, N65–N70. [[CrossRef](#)]
133. Diez, E.; Perez, H.; Marquez, J.; Vizan, A. Feasibility study of in-process compensation of deformations in flexible milling. *Int. J. Mach. Tools Manuf.* **2015**, *94*, 1–14. [[CrossRef](#)]
134. Rashid, A.; Mihai Nicolescu, C. Active vibration control in palletised workholding system for milling. *Int. J. Mach. Tools Manuf.* **2006**, *46*, 1626–1636. [[CrossRef](#)]
135. Yang, Y.; Xu, D.; Liu, Q. Milling vibration attenuation by eddy current damping. *Int. J. Adv. Manuf. Technol.* **2015**, *81*, 445–454. [[CrossRef](#)]
136. Yang, Y.; Xie, R.; Liu, Q. Design of a passive damper with tunable stiffness and its application in thin-walled part milling. *Int. J. Adv. Manuf. Technol.* **2017**, *89*, 2713–2720. [[CrossRef](#)]
137. Díaz-Tena, E.; Marcaide, L.N.L.D.L.; Gómez, F.J.C.; Bocanegra, D.L.C. Use of Magnetorheological Fluids for Vibration Reduction on the Milling of Thin Floor Parts. *Procedia Eng.* **2013**, *63*, 835–842. [[CrossRef](#)]
138. Wang, T.; Zha, J.; Jia, Q.; Chen, Y. Application of low-melting alloy in the fixture for machining aeronautical thin-walled component. *Int. J. Adv. Manuf. Technol.* **2016**, *87*, 2797–2807. [[CrossRef](#)]
139. Kolluru, K.V.; Axinte, D.A.; Raffles, M.H.; Becker, A.A. Vibration suppression and coupled interaction study in milling of thin wall casings in the presence of tuned mass dampers. *Proc. Inst. Mech. Eng. Part B J. Eng. Manuf.* **2013**, *228*, 826–836. [[CrossRef](#)]
140. Woody, S.C.; Smith, S.T. Damping of a thin-walled honeycomb structure using energy absorbing foam. *J. Sound Vib.* **2006**, *291*, 491–502. [[CrossRef](#)]
141. Garimella, S.; Ramesh Babu, P. Understanding the challenges in machining thin walled thin floored Avionics components. *Int. J. Appl. Sci. Eng. Res.* **2013**, *2*, 93–100.
142. Izamshah, R.A.; Mo, J.P.T.; Ding, S. Hybrid deflection prediction on machining thin-wall monolithic aerospace components. *Proc. Inst. Mech. Eng. Part B J. Eng. Manuf.* **2011**, *226*, 592–605. [[CrossRef](#)]
143. Khandagale, P.; Bhakar, G.; Kartik, V.; Joshi, S.S. Modelling time-domain vibratory deflection response of thin-walled cantilever workpieces during flank milling. *J. Manuf. Process.* **2018**, *33*, 278–290. [[CrossRef](#)]
144. Zhang, L.; Gao, W.; Zhang, D.; Tian, Y. Prediction of Dynamic Milling Stability considering Time Variation of Deflection and Dynamic Characteristics in Thin-Walled Component Milling Process. *Shock Vib.* **2016**, *2016*, 3984186. [[CrossRef](#)]
145. Scheider, I.; Brocks, W. Residual strength prediction of a complex structure using crack extension analyses. *Eng. Fract. Mech.* **2009**, *76*, 149–163. [[CrossRef](#)]
146. Mahmud, A.; Mayer, J.R.R.; Baron, L. Determining the minimum clamping force by cutting force simulation in aerospace fuselage pocket machining. *Int. J. Adv. Manuf. Technol.* **2015**, *80*, 1751–1758. [[CrossRef](#)]
147. Panczuk, R. Clean alternative technology to chemical milling: Demonstration of technical, environmental and economic performance of mechanical milling for the machining of complex shaped panels used in the aeronautical and space industries—GAP (Green Advanced Panel). 2007. Available online: [https://nanopdf.com/download/gap-clean-alternative-technology-to-chemical-milling\\_pdf](https://nanopdf.com/download/gap-clean-alternative-technology-to-chemical-milling_pdf) (accessed on 25 June 2018).
148. Jiang, X.; Lu, W.; Zhang, Z. An approach for improving the machining efficiency and quality of aerospace curved thin-walled parts during five-axis NC machining. *Int. J. Adv. Manuf. Technol.* **2018**, *97*, 2477–2488. [[CrossRef](#)]
149. Urbikain, G.; Olvera, D.; de Lacalle, L.N.L. Stability contour maps with barrel cutters considering the tool orientation. *Int. J. Adv. Manuf. Technol.* **2017**, *89*, 2491–2501. [[CrossRef](#)]
150. Zhang, X.; Yu, T.; Wang, W.; Ehmann, K.F. Three-dimensional process stability prediction of thin-walled workpiece in milling operation. *Mach. Sci. Technol.* **2016**, *20*, 406–424. [[CrossRef](#)]
151. Meshreki, M.; Attia, H.; Kövecses, J. Development of a New Model for the Varying Dynamics of Flexible Pocket-Structures During Machining. *J. Manuf. Sci. Eng.* **2011**, *133*, 041002. [[CrossRef](#)]

152. Fernández, B.; González, B.; Artola, G.; López de Lacalle, N.; Angulo, C. A Quick Cycle Time Sensitivity Analysis of Boron Steel Hot Stamping. *Metals* **2019**, *9*, 235. [[CrossRef](#)]
153. Calleja, A.; Bo, P.; Gonzalez, H.; Bartoň, M.; López de Lacalle, L.N. Highly accurate 5-axis flank CNC machining with conical tools. *Int. J. Adv. Manuf. Technol.* **2018**, *97*, 1605–1615.



© 2019 by the authors. Licensee MDPI, Basel, Switzerland. This article is an open access article distributed under the terms and conditions of the Creative Commons Attribution (CC BY) license (<http://creativecommons.org/licenses/by/4.0/>).

## **Appendix B:**

*Effects of Machining Parameters on the Quality in  
Machining of Aluminium Alloys Thin Plates*

## Article

# Effects of Machining Parameters on the Quality in Machining of Aluminium Alloys Thin Plates

Irene Del Sol <sup>1,\*</sup> , Asuncion Rivero <sup>2</sup> and Antonio J. Gamez <sup>1</sup>

<sup>1</sup> Department of Mechanical Engineering and Industrial Design, School of Engineering, University of Cadiz, Av. Universidad de Cádiz 10, Puerto Real (Cádiz) E-11519, Spain

<sup>2</sup> Fundación Tecnalia Research & Innovation, Scientific and Technological Park of Guipuzkoa, Paseo Mikeletegui, Donostia-San Sebastián (Guipuzcoa) 7 E-20009, Spain

\* Correspondence: irene.delsol@uca.es; Tel.: +34-956-483-513

Received: 23 July 2019; Accepted: 22 August 2019; Published: 24 August 2019



**Abstract:** Nowadays, the industry looks for sustainable processes to ensure a more environmentally friendly production. For that reason, more and more aeronautical companies are replacing chemical milling in the manufacture of skin panels and thin plates components. This is a challenging operation that requires meeting tight dimensional tolerances and differs from a rigid body machining due to the low stiffness of the part. In order to fill the gap of literature research on this field, this work proposes an experimental study of the effect of the depth of cut, the feed rate and the cutting speed on the quality characteristics of the machined parts and on the cutting forces produced during the process. Whereas surface roughness values meet the specifications for all the machining conditions, an appropriate cutting parameters selection is likely to lead to a reduction of the final thickness deviation by up to 40% and the average cutting forces by up to a 20%, which consequently eases the clamping system and reduces machine consumption. Finally, an experimental model to control the process quality based on monitoring the machine power consumption is proposed.

**Keywords:** thin plates; thin-wall; machining; aluminium; cutting forces; roughness

## 1. Introduction

Aluminium fuselage skin panel machining is considered a challenging operation due to its dimensional and surface requirements. These parts are lightened by machining superficial pockets in order to increase the fuel efficiency of aircrafts by reducing their structure weight. These pockets have historically been machined using chemical milling operations, although green manufacturing approaches have been focused on the study of mechanical machining for this purpose [1]. In fact, different projects and research studies have invested hundreds of thousands of euros to remove chemical milling, designing specific clamping systems to ensure surface quality and dimensional requirements while maintaining clamping flexibility. These systems are focused on twin-machining heads [2,3], magnetic slaves [4] or flexible vacuum beds [5] that control the deflection of the part avoiding overcut during the operation.

Additionally, the conventional machining of low stiffness parts presents dynamic and static problems [6,7]. On the one hand, dynamic stability of machining strongly depends on system stiffness, its natural frequency response, and the selected cutting parameters. Vibrations—chatter and forced vibrations—can directly affect the final roughness of parts, increasing their value and forcing manufacturers to make reprocessing steps, therefore increasing the operational cost [8,9]. In order to avoid them, chatter influence is studied using stability lobe diagrams (SLD), a representation tool that commonly relates the stability areas of machining with the feed rate, the spindle speed, the depth of cut, or the tool position [10–14], and forced vibrations can be studied through dynamic models. In this

case, the applied force is studied to reduce the dynamic deflection of the part. On the other hand, quasi-static deflection can take place when the elastoplastic behaviour of the workpiece, combined with a failure on the clamping, is not enough to counter the machining force effect, reducing the real depth of cut [15–17]. This fact was proved experimentally by Yan et al. [18], who optimized the depth of cut depending on the cutting force, reducing the part deflection and increasing the process efficiency. Similarly, Sonawane et al. [19] used a statistical approach to model workpiece deflection, addressing it to the machining parameters and cutting tool orientation. In contrast, Oliveira et al. [20] established that the most influencing factor on the real depth of cut was the milling strategy (up or down milling), while other studies [21,22] have focused on the analysis of the toolpath effect on the final quality of slim parts.

However, few studies have been focused on the analysis of the parameters effect into the quality characteristics of thin plates. The literature review has shown that most of the studies have focused on thin-wall machining rather than thin-plates or thin floors [7]. Few of them have focused on the analysis of the parameters effect into the final quality characteristics. For this reason, this paper focuses on the study of thin plates in order to simulate the machining of large skin panels to evaluate the effect of the machining parameters on the final thickness, surface roughness and cutting forces of the part.

## 2. Materials and Methods

### 2.1. Machining Tests

Two type of machining tests were performed. The first type was used to analyse the thin plates' behaviour through the machining of  $50 \times 50 \text{ mm}^2$  pockets on samples of  $80 \times 80 \text{ mm}^2$  and 2 mm thickness. Parts were screwed to a faced mill plate that was housed on a dynamometer. The samples were dry machined while keeping the axial distance constant, and the depth of cut ( $a_p$ ), the feed rate per tooth ( $f_z$ ) and the cutting speed ( $V_c$ ) were variable. The values of each machining conditions are compiled in the levels listed in Table 1, in which the spindle speed ( $S$ ) is also shown. The depth of cut was selected based on the geometrical requirements of industrial parts. Feed rate and cutting speed were selected based on the literature [14,23,24] and aerospace recommendations. The chosen strategy was down milling, following a toolpath from the centre of the workpiece up to the outside of it.

**Table 1.** Machining parameters and levels for skin sample tests.

Parameter	Level 1	Level 2	Level 3	Level 4
$a_p$ (mm)	0.2	0.4	0.8	1.0
$f_z$ (mm/tooth)	0.08	0.1	-	-
$S$ (rpm)	4,000	12,000	18,000	-
$V_c$ (m/min)	126	378	566	-

The second test aimed to obtain the cutting force values following a mechanistic approach. In this approach, the specific force coefficients of the combination pair tool-material had to be experimentally defined by performing different slots on a rigid aluminium workpiece. Additionally, in order to avoid chatter and ensure the rigid behaviour of the samples, SLD were calculated using an impact hammer test. The maximum depth of cut for stable machining was calculated using the procedure described by Altintas and Budak [25]. Following this procedure, the frequency responses of the tool and the workpiece at four different steps of the cutting operation were obtained. This combination provided the SLD diagram at the four stages in order to analyse possible changes during the machining operation.

Each machining test was performed in a 5-axis NC centre ZV 25U600 EXTREME (Ibarmia Innovatek S.L.U., Azkoitia, Spain). The material used on the sample parts was aluminium 2024-T3, and the tool was a torus end mill KENDU 4400.60 (Kendu, Segura, Spain) with a 10 mm diameter,  $30^\circ$  helix angle,  $18^\circ$  rake angle,  $16^\circ$  clearance angle for the secondary edge and  $9^\circ$  angle for the primary edge.

Forces and accelerations on the workpiece were monitored using a dynamometer Kistler 9257B (Kistler Group, Winterthur, Switzerland) and an accelerometer Kistler 8728A500 (Kistler Group, Winterthur, Switzerland), connected to National Instruments acquisition boards NI 9215 (National Instruments, Austin, TX, USA) and NI 9234 (National Instruments, Austin, TX, USA), respectively. The power consumed by the spindle speed and the whole machine was also recorded using a Fanuc Servoguide system (Fanuc Corporation, Oshino-mura, Japan). The test configuration and monitoring system are shown in Figure 1.

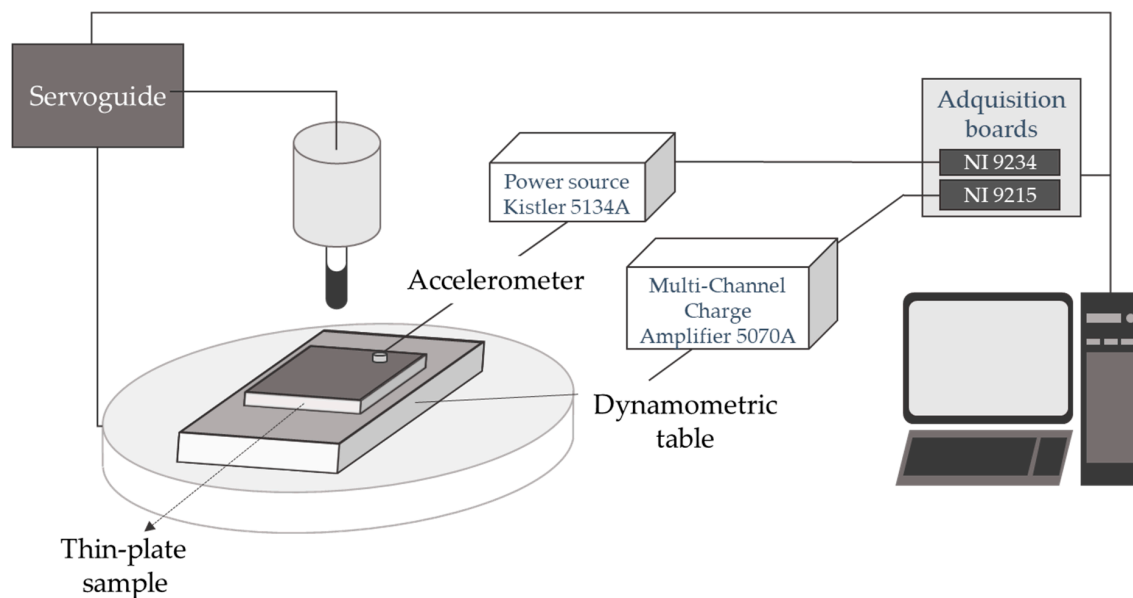


Figure 1. Scheme of the monitoring system.

## 2.2. Force Mechanistic Model

The expected forces could be calculated through a mechanistic approach [26,27]. Tangential ( $t$ ), axial ( $a$ ) and radial ( $r$ ) forces could be considered as a function of the cutting coefficient ( $K_{qc}$ ) and the friction coefficient ( $K_{qe}$ ).

$$\partial F_q(\varphi, z) = K_{qe} \partial S + K_{qc} f_z \sin \varphi(\varphi_i, z) \partial z, \quad q = \{t, r, a\} \quad (1)$$

where  $\partial S$  is the differential chip edge length and  $\varphi$  is the applied rotation angle which depends on the instant depth of cut ( $z$ ), the number of teeth engaged ( $j$ ), the total number of teeth ( $N$ ), and the helix angle ( $\beta$ ).

$$\varphi(\varphi_i, z) = \varphi_i - (j - 1) \frac{2\pi}{N} - \beta \quad (2)$$

The cutting forces were converted to Cartesian coordinates using Equation (3), with  $\kappa$  being the angle referred to the torus part of the mill.

$$\frac{\partial F_{x,y,z}}{\partial z} = \begin{bmatrix} -\cos \varphi & -\sin \varphi \sin \kappa & -\sin \varphi \cos \kappa \\ \sin \varphi & -\cos \varphi \sin \kappa & -\cos \varphi \cos \kappa \\ 0 & \cos \kappa & -\sin \kappa \end{bmatrix} \begin{bmatrix} \partial F_t \\ \partial F_r \\ \partial F_a \end{bmatrix} \quad (3)$$

The cutting and friction coefficients were obtained by solving the equation using the force values obtained in the slot test performed in a rigid part. The coefficients were considered constant for all the  $f_z$ , but the effect of the  $V_c$  was taken into account. The test conditions are shown in Table 2. The results were used to predict the SLD.



**Table 2.** Machining parameters and levels for cutting coefficient calculation tests.

Parameter	Level 1	Level 2	Level 3
$a_p$ (mm)	0.2	0.6	1.0
$f_z$ (mm/tooth)	0.06	0.08	0.1
$S$ (rpm)	4,000	12,000	18,000
$V_c$ (m/min)	126	378	566

### 2.3. Quality Evaluation

The quality of the parts was established through the final thickness distribution and roughness. Typical tolerance values in the industry were really tight, about  $\pm 0.1$  mm for final thickness and under  $1.6 \mu\text{m}$  for the roughness average ( $R_a$ ).

Final thicknesses were measured using a single coordinate measurement machine with an electronic comparator set. Nine points of the sample were evaluated, as shown in Figure 2a.  $R_a$  was measured using a Mahr Perthometer Concept PGK120 roughness measure station (Mahr technology, Göttingen, Germany) on five different areas of the part (Figure 2b). The areas for the roughness measures were selected in order to study the whole machining process and to cover both machine  $x$  and  $y$  axes. Roughness measurements were taken following the standard ISO 4288:1996 [28].

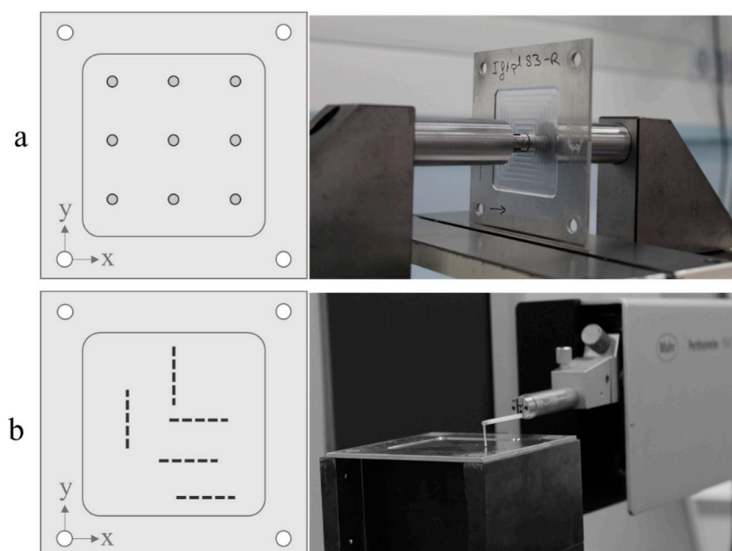


**Figure 2.** Measure procedure. (a) points selected for the thickness analysis and (b) areas studied for the roughness analysis.

## 3. Results and Discussion

### 3.1. Final Thickness Error

The final thickness error can be defined as the difference between the experimental thickness and the expected one; this parameter measures the real part dimension. In addition to the static and dynamic phenomena that occur during low rigidity parts machining [7], aspects such as the machine positioning error and the thermal expansion of the spindle have influence over this parameter. Other possible thermal errors can be discarded due to the short length of the machining test, which allowed us to underestimate the effect on the accuracy of the machine due to temperature changes in its surroundings.

The analysis of the results showed that the feed rate had a negligible effect on the average final thickness error, while the cutting speed seems to have had a significant effect on this parameter. The higher the cutting speed, the greater the geometric error was, and the piece became thinner (Figure 3).



Nevertheless, the thermal expansion of the spindle increased with the revolutions and therefore with the cutting speed [29]. This fact explains the part thinning, rejecting the direct effect of the cutting speed. Though the thermal expansion of the spindle was identified as an influencing parameter for the increase of the final average thickness error of the part, this error was easy to compensate when studying the elongation curves of the spindle and considering them in the CAM design [30] or implementing error compensation rules in the machine control [5].

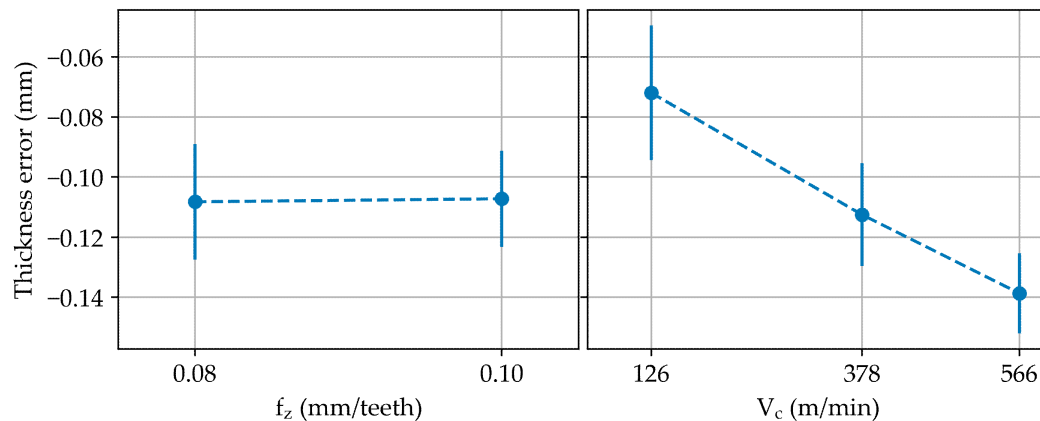


**Figure 3.** Average final thickness error depending on the feed per tooth ( $f_z$ ) and the cutting speed ( $V_c$ ).

Once the average error—not directly related to the cutting parameters—can be compensated, the target is to get a homogeneous thickness distribution. Higher values of feeds per teeth combined with higher values of spindle speed led to a reduction up to 40% of the standard deviation of the thickness errors measured in a test sample. This decrease was due to a better behaviour of the process in terms of dynamics. If the part was machined at higher rotation speed where cutting forces excited higher frequency vibration modes and created lower vibration amplitudes (Figure 4), therefore leading to a more homogeneous thickness distribution

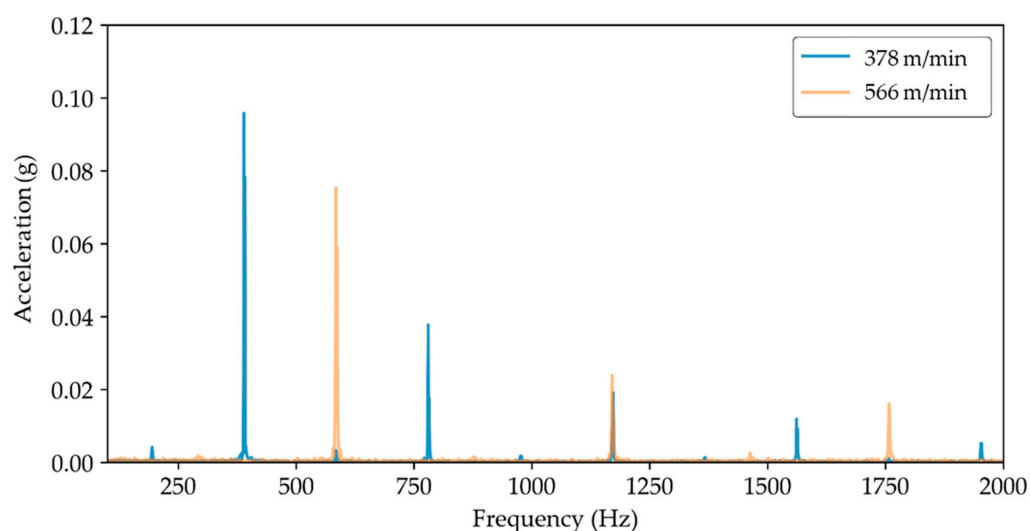


**Figure 4.** Fast Fourier Transform of the part acceleration signal for test at  $f_z = 0.1$  and  $a_p = 1.0$  mm, under two different cutting speeds.

### 3.2. Roughness

Roughness results were not significantly affected by any of the studied parameters in average deviation, with all of them being inside the most restrictive tolerance values ( $1.6 \mu\text{m}$ ) required in chemical milling process (Figure 5a).

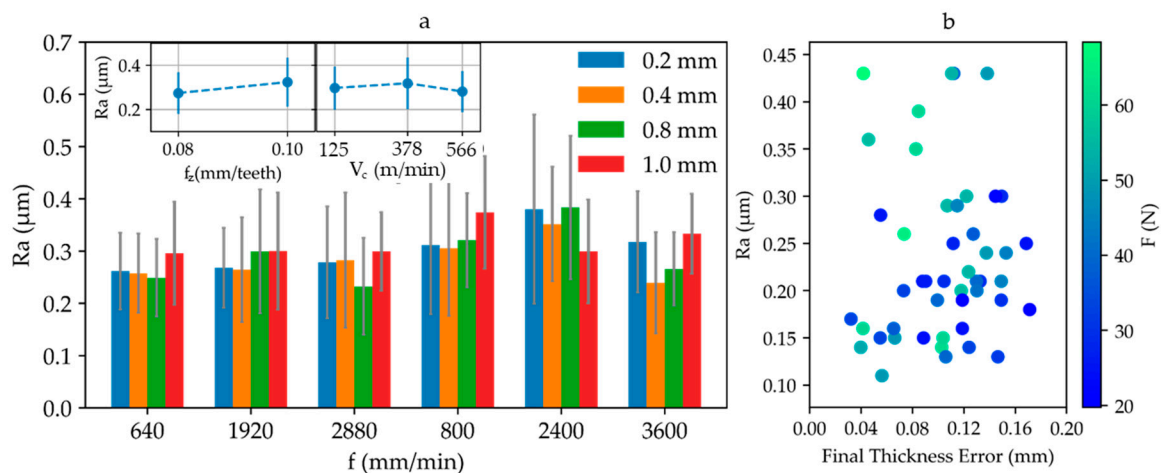


**Figure 5.** (a) Average of the roughness values obtained for different feed rates ( $f = N \cdot f_z \cdot S$ ) as a function of the depth of cut. The inset shows the partial effect of the feed rate per teeth and the cutting speed. (b) Average roughness values of each performed test against the depth of cut error considering the force module.

Measured forces and depths of cut errors did not have any impact on this quality characteristic (Figure 5b). However, lower cutting force values were related to roughness values under  $0.3 \mu\text{m}$ . In fact, lower forces caused less tool deflection and vibrations of smaller amplitudes, leading to more stable machining processes that allowed us to produce more homogenous surfaces [31]. This revealed that the surface quality can be kept constant for any depth of cut under similar machining conditions. For this reason, the selection of parameters that decrease the forces should be considered.

### 3.3. Forces and Power Models

According to the SLD (Figure 6), thin plates almost behaved like a rigid part. This fact ensures that the tests were performed under stable machining conditions, proving that any variation occurring on the final thickness of the part was not produced by chatter issues.

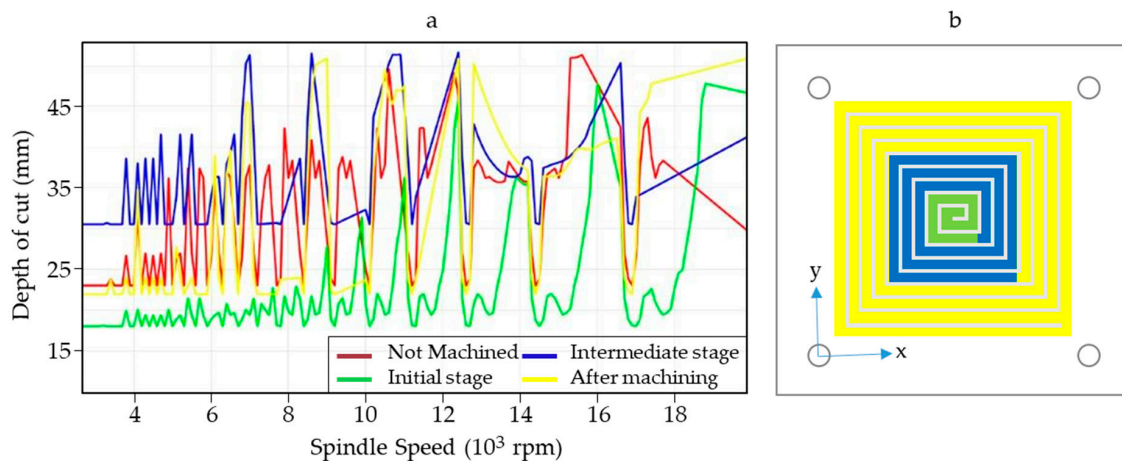


**Figure 6.** (a) Stability Lobe Diagrams (SLD) variation depending on the machining stage. Red line, before the machining; green line, in the first instants of the machining; blue line, intermediate stage; and yellow line, after the whole machining operation was performed. (b) Scheme of the areas of material removed in each stage with corresponding colours.

However, the forces obtained on the tests performed on a rigid body did not completely agree with those measured on the flexible parts (Figure 7). The depth of cut was linearly related to  $F_x$  and  $F_y$ ,

but for medium and high cutting speed values, the  $F_z$  initiated a constant trend at cutting depths of 0.8 and 0.1 mm, respectively. Even though the machining operation was not in a high speed machining regimen for aluminium alloys, there was a decrease of the force values expected for the higher depths of cut. This fact had been previously observed by López de Lacalle et al. [32], where, due to the reduction of stiffness, the cutting forces decreased, obtaining behaviours closer to high speed machining at lower cutting speed.

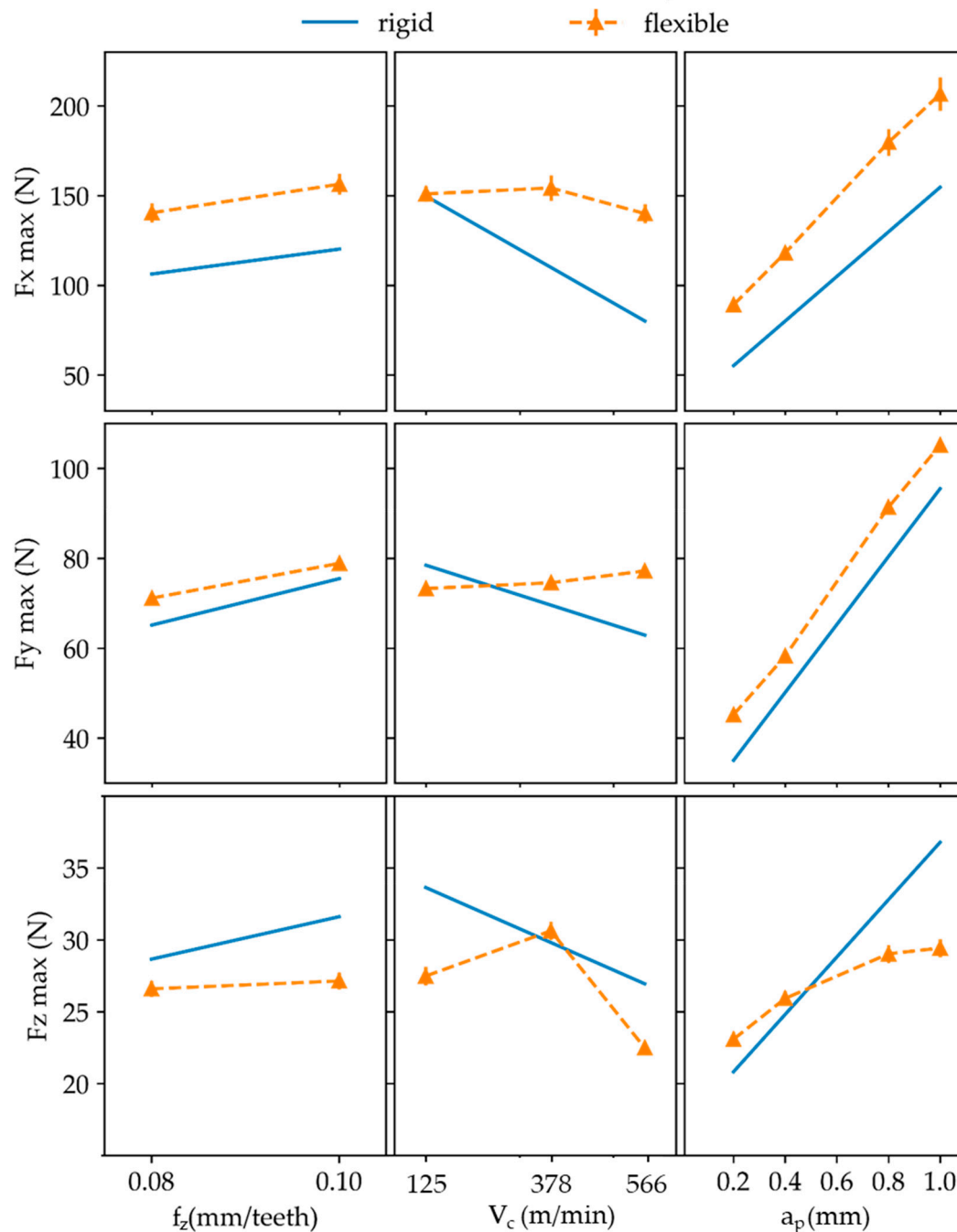


**Figure 7.** Average forces for the  $x$ ,  $y$  and  $z$  axes under rigid (solid blue line) and flexible (dashed orange line) consideration.

Aiming to provide a suitable model to relate the machining parameters to the process performance, the forces have been also studied by following a statistical approach. In this research, the force

module and the material removal rate (*MRR*), which can be calculated as is shown in Equation (4), were correlated.

$$MRR = f_z \cdot S \cdot a_p \cdot N \cdot a_r \quad (4)$$

A potential regression was chosen for the model in order to ensure an  $R^2$  close to 0.95. The model equation is shown in Equation (5), where  $e$  is the Euler number,  $N$  is the number of teeth and  $a_r$  is the radial depth of cut.

$$F = MRR^{0.63} e^{-0.44-7.78 \cdot 5 \cdot 10^{-5}} \quad (5)$$

This model relates the force module ( $F$ ) to the machining parameters through the *MRR*, and, as such, the concept of process productivity is introduced. This approach makes it easier to select higher efficient parameters. Both experimental and predicted data are shown in Figure 8. The reduction of forces at high spindle speeds for the same *MRR* is remarkable. This fact can be explained by a working regime close to high speed machining, as was referred to in previous paragraphs. The increase of the process temperature reduced the effort needed to cut the material [33]. Additionally, the heat generated in the process was quickly evacuated, which could have reduced induced residual stresses [34] and tool wear [33].

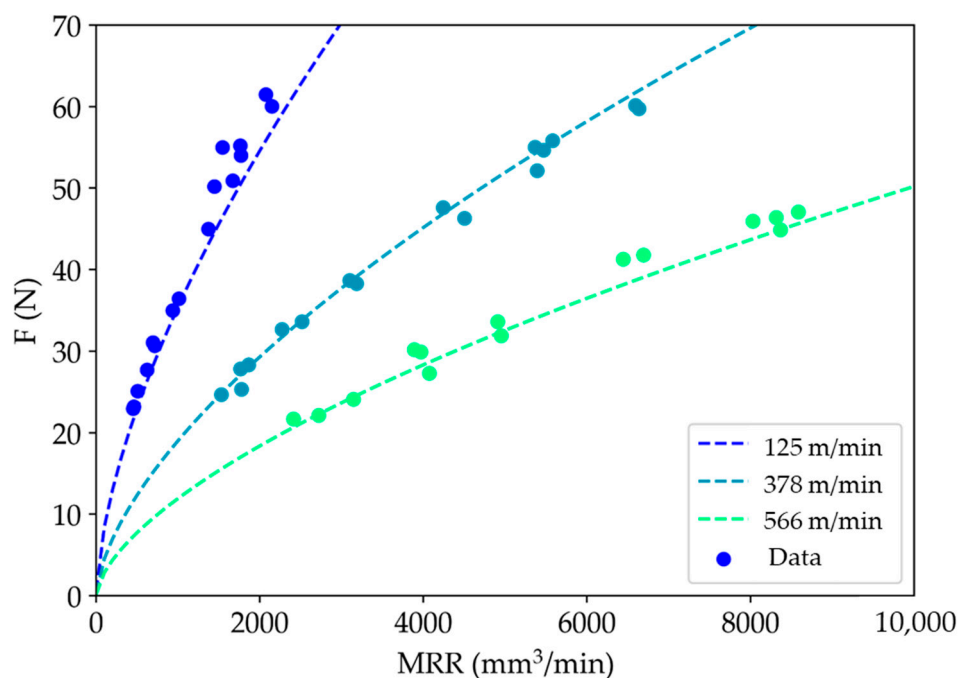


**Figure 8.** Average force module predicted (dashed lines) and experimental data against the material removal rate (*MRR*) as a function of the cutting speed ( $V_c$ ).

The force predicted by the proposed model, as a function of the cutting parameters, allowed the machining operation to be monitored using the electrical power registered by the ServoGuide System. Machining cutting power involved all the cutting parameters together, thus giving a closer idea of the overall interactions in the cutting process [35]. This monitoring option could be used as an input for adaptive control systems, in which the instant depth of cut can be controlled and modified online, as an alternative to others online depth of cut control based on ultrasound measurements [36]. This can reduce the number of overcuts and defective parts produced. In this case, the empirical model followed Equation (4), where  $e$  is the Euler number and  $D$  the tool diameter.

$$Power = \left( \frac{F \cdot S \cdot D \cdot \pi}{60} \right)^{3.5} a_p^{-2.2} e^{-16.7} \quad (6)$$

This equation was empirically obtained following an ANOVA approach, using the data represented on Figure 9. Combined relations between the different variables were neglected during the analysis. The  $R^2$  for the final statistical model was 0.953.

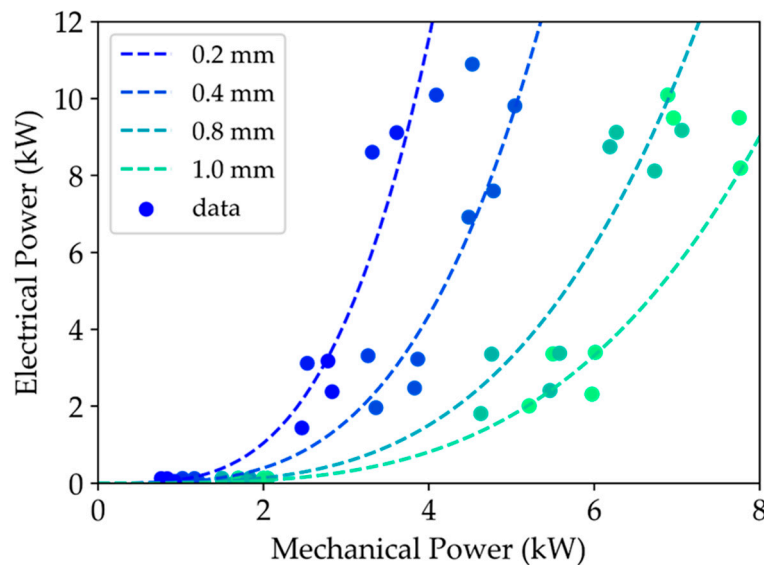


**Figure 9.** Model correlation between the mechanical power, calculated based on the recorded forces, and the electrical power obtained on the ServoGuide system as a function of the  $a_p$ .

#### 4. Conclusions

The machining of aluminium skin panels is used as a sustainable alternative for chemical milling process in the aerospace industry; therefore, it requires tight quality tolerances. This work presents a study of how cutting parameters influence the final thickness, surface roughness and cutting forces of thin plate aluminium parts in order to pursue two main objectives: To ensure the final quality of the part and to find an easy way to monitor the process.

The influence of the cutting speed on the final thickness error map of the machined thin plates has been proven. Higher values of cutting speeds tended to reduce the standard deviation of thickness error values measured in the test samples. The higher the cutting speed, the lower the cutting force module and the higher its excitation frequency, leading to an increase of process stability and a reduction of the results variability. Consequently, an improvement by up to a 40% of the implicit process tolerances has been achieved using a cutting speed of 566 m/min. This fact suggests that these parts could present even more homogenous results in terms of final thickness if higher cutting speeds were used. Roughness values are always under the more restrictive requirements for chemical milling. Lower values of cutting forces under stable machining conditions could ensure roughness values under  $0.3 \mu\text{m}$ .

Furthermore, forces are affected by the low rigidity of the part that obtain lower average values for the  $z$  axis than those expected, based on rigid body experiments. A statistical analysis of the tests also revealed high cutting speed parameters as the more efficient ones based on  $MRR$ , providing a force model that includes all cutting parameter effects.

Finally, this model was used to relate mechanical power and electrical power consumption, allowing us to control online the depth of cut. This model is proposed as an alternative method to implement adaptive control techniques in order to avoid overcuts on aeronautical panels, reducing defective parts at the final stages of the process chain when their value is very high.

**Author Contributions:** Conceptualization, I.D.S., A.R. and A.J.G.; methodology, I.D.S. and A.R.; formal analysis, I.D.S. and A.J.G.; investigation, I.D.S. and A.R.; resources, A.R.; writing—original draft preparation, I.D.S.; writing—review and editing, A.R. and A.J.G.

**Funding:** This research was funded by University of Cadiz, grant number University training plan UCA/REC01VI/2016.

**Acknowledgments:** The authors acknowledge the support given by the Fraunhofer Joint Laboratory of Excellence on Advanced Production Technology (Fh-J\_LEAPT Naples).

**Conflicts of Interest:** The authors declare no conflict of interest.

## References

1. Bi, Q.; Huang, N.; Zhang, S.; Shuai, C.; Wang, Y. Adaptive machining for curved contour on deformed large skin based on on-machine measurement and isometric mapping. *Int. J. Mach. Tools Manuf.* **2019**, *136*, 34–44. [CrossRef]
2. Mtorres Surface Milling Machining. Available online: <http://www.mtorres.es/en/aeronautics/products/metallic/torres-surface-milling> (accessed on 2 June 2016).
3. Dufieux Dufieux Industrie—Modular. Available online: <http://www.dufieux-industrie.com/en/mirror-milling-system-mms> (accessed on 2 June 2016).
4. Mahmud, A.; Mayer, J.R.R.; Baron, L. Magnetic attraction forces between permanent magnet group arrays in a mobile magnetic clamp for pocket machining. *CIRP J. Manuf. Sci. Technol.* **2015**, *11*, 82–88. [CrossRef]
5. Rubio, A.; Rivero, A.; Del Sol, I.; Ukar, E.; Lamikiz, A.; Rubio-Mateos, A.; Rivero-Rastrero, A.; Del Sol-Illana, I.; Ukar-Arrien, E.; Lamikiz-Mentxaka, A. Capacitation of flexibles fixtures for its use in high quality machining processes: An application case of the Industry 4.0 paradigm. *DYNA* **2018**, *93*, 608–612. [CrossRef]
6. Campa, F.J.; López de Lacalle, L.N.; Celaya, A. Chatter avoidance in the milling of thin floors with bull-nose end mills: Model and stability diagrams. *Int. J. Mach. Tools Manuf.* **2011**, *51*, 43–53. [CrossRef]
7. Del Sol, I.; Rivero, A.; Norberto, L.; Gamez, A.J. Thin-Wall Machining of Light Alloys: A Review of Models and Industrial Approaches. *Materials* **2019**, *12*, 2012. [CrossRef] [PubMed]
8. Elbestawi, M.A.; Sagherian, R. Dynamic modeling for the prediction of surface errors in the milling of thin-walled sections. *J. Mater. Process. Technol.* **1991**, *25*, 215–228. [CrossRef]
9. Tian, W.; Ren, J.; Wang, D.; Zhang, B. Optimization of non-uniform allowance process of thin-walled parts based on eigenvalue sensitivity. *Int. J. Adv. Manuf. Technol.* **2018**, *96*, 2101–2116. [CrossRef]
10. Olvera, D.; Urbikain, G.; Elías-Zuñiga, A.; López de Lacalle, L. Improving Stability Prediction in Peripheral Milling of Al7075T6. *Appl. Sci.* **2018**, *8*, 1316. [CrossRef]
11. Urbikain, G.; Olvera, D.; de Lacalle, L.N.L. Stability contour maps with barrel cutters considering the tool orientation. *Int. J. Adv. Manuf. Technol.* **2017**, *89*, 2491–2501. [CrossRef]
12. Liu, X.; Gao, H.; Yue, C.; Li, R.; Jiang, N.; Yang, L. Investigation of the milling stability based on modified variable cutting force coefficients. *Int. J. Adv. Manuf. Technol.* **2018**, *96*, 2991–3002. [CrossRef]
13. Qu, S.; Zhao, J.; Wang, T. Three-dimensional stability prediction and chatter analysis in milling of thin-walled plate. *Int. J. Adv. Manuf. Technol.* **2016**, *86*, 2291–2300. [CrossRef]
14. Campa, F.J.; López de Lacalle, L.N.; Lamikiz, A.; Sánchez, J.A. Selection of cutting conditions for a stable milling of flexible parts with bull-nose end mills. *J. Mater. Process. Technol.* **2007**, *191*, 279–282. [CrossRef]
15. Ding, H.; Ke, Y. Study on Machining Deformation of Aircraft Monolithic Component by FEM and Experiment. *Chinese J. Aeronaut.* **2006**, *19*, 247–254. [CrossRef]
16. Tuysuz, O.; Altintas, Y. Frequency Domain Updating of Thin-Walled Workpiece Dynamics Using Reduced Order Substructuring Method in Machining. *J. Manuf. Sci. Eng.* **2017**, *139*, 071013. [CrossRef]
17. Lin, X.; Wu, D.; Yang, B.; Wu, G.; Shan, X.; Xiao, Q.; Hu, L.; Yu, J. Research on the mechanism of milling surface waviness formation in thin-walled blades. *Int. J. Adv. Manuf. Technol.* **2017**, *93*, 2459–2470. [CrossRef]
18. Yan, Q.; Luo, M.; Tang, K. Multi-axis variable depth-of-cut machining of thin-walled workpieces based on the workpiece deflection constraint. *CAD Comput. Aided Des.* **2018**, *100*, 14–29. [CrossRef]
19. Sonawane, H.A.; Joshi, S.S. Modeling of machined surface quality in high-speed ball-end milling of Inconel-718 thin cantilevers. *Int. J. Adv. Manuf. Technol.* **2015**, *78*, 1751–1768. [CrossRef]



20. De Oliveira, E.L.; de Souza, A.F.; Diniz, A.E. Evaluating the influences of the cutting parameters on the surface roughness and form errors in 4-axis milling of thin-walled free-form parts of AISI H13 steel. *J. Braz. Soc. Mech. Sci. Eng.* **2018**, *40*, 334. [\[CrossRef\]](#)
21. Del Sol, I.; Rivero, A.; Salguero, J.; Fernández-Vidal, S.R.; Marcos, M. Tool-path effect on the geometric deviations in the machining of UNS A92024 aeronautic skins. *Procedia Manuf.* **2017**, *13*, 639–646. [\[CrossRef\]](#)
22. Seguy, S.; Campa, F.J.; López de Lacalle, L.N.; Arnaud, L.; Dessein, G.; Aramendi, G. Toolpath dependent stability lobes for the milling of thin-walled parts. *Int. J. Mach. Mach. Mater.* **2008**, *4*, 377–392. [\[CrossRef\]](#)
23. Mahmud, A.; Mayer, J.R.R.; Baron, L. Determining the minimum clamping force by cutting force simulation in aerospace fuselage pocket machining. *Int. J. Adv. Manuf. Technol.* **2015**, *80*, 1751–1758. [\[CrossRef\]](#)
24. Li, B.; Jiang, X.; Yang, J.; Liang, S.Y. Effects of depth of cut on the redistribution of residual stress and distortion during the milling of thin-walled part. *J. Mater. Process. Technol.* **2015**, *216*, 223–233. [\[CrossRef\]](#)
25. Altıntaş, Y.; Budak, E. Analytical Prediction of Stability Lobes in Milling. *CIRP Ann. Manuf. Technol.* **1995**, *44*, 357–362. [\[CrossRef\]](#)
26. Budak, E. Analytical models for high performance milling. Part I: Cutting forces, structural deformations and tolerance integrity. *Int. J. Mach. Tools Manuf.* **2006**, *46*, 1478–1488. [\[CrossRef\]](#)
27. Gradišek, J.; Kalveram, M.; Weinert, K. Mechanistic identification of specific force coefficients for a general end mill. *Int. J. Mach. Tools Manuf.* **2004**, *44*, 401–414. [\[CrossRef\]](#)
28. ISO, EN. 4288—Geometrical Product Specifications (GPS)—Surface Texture: Profile Method—Rules and Procedures for the Assessment of Surface Texture; International Organization for Standardization: Geneva, Switzerland, 1996.
29. Chen, J.S.; Hsu, W.Y. Characterizations and models for the thermal growth of a motorized high speed spindle. *Int. J. Mach. Tools Manuf.* **2003**, *43*, 1163–1170. [\[CrossRef\]](#)
30. Ratchev, S.; Liu, S.; Huang, W.; Becker, A.A. Milling error prediction and compensation in machining of low-rigidity parts. *Int. J. Mach. Tools Manuf.* **2004**, *44*, 1629–1641. [\[CrossRef\]](#)
31. Bolar, G.; Das, A.; Joshi, S.N. Measurement and analysis of cutting force and product surface quality during end-milling of thin-wall components. *Meas. J. Int. Meas. Confed.* **2018**, *121*, 190–204. [\[CrossRef\]](#)
32. López De Lacalle, L.N.; Lamikiz, A.; Sánchez, J.A.; Bustos, I.F. de Recording of real cutting forces along the milling of complex parts. *Mechatronics* **2006**, *16*, 21–32. [\[CrossRef\]](#)
33. Brinksmeier, E.; Preuss, W.; Riemer, O.; Rentsch, R. Cutting forces, tool wear and surface finish in high speed diamond machining. *Precis. Eng.* **2017**, *49*, 293–304. [\[CrossRef\]](#)
34. Masoudi, S.; Amini, S.; Saeidi, E.; Eslami-Chalander, H. Effect of machining-induced residual stress on the distortion of thin-walled parts. *Int. J. Adv. Manuf. Technol.* **2014**, *76*, 597–608. [\[CrossRef\]](#)
35. Ma, Y.; Feng, P.; Zhang, J.; Wu, Z.; Yu, D. Energy criteria for machining-induced residual stresses in face milling and their relation with cutting power. *Int. J. Adv. Manuf. Technol.* **2015**, *81*, 1023–1032. [\[CrossRef\]](#)
36. Rubio, A.; Calleja, L.; Orive, J.; Mújica, Á.; Rivero, A. Flexible Machining System for an Efficient Skin Machining. *SAE Int.* **2016**, *1–12*. [\[CrossRef\]](#)



## **Appendix C:**

*Tribological performance of ionic liquids as  
additives of water-based cutting fluids*



I. Del Sol, A.J. Gámez, A. Rivero and P. Iglesias

*Tribological performance of ionic liquids as additives of water-based cutting fluids*

Wear 426–427 (2019), pp. 845–852.

DOI: <https://doi.org/10.1016/j.wear.2019.01.109>

**Abstract:**

Dry machining of aluminum parts has been the most eco-friendly method in an attempt to reduce the use of mineral-based lubricants and other working fluids. The drawbacks of dry machining include an increase of contact temperatures and stresses leading to high values of tool wear and a decrease of the tool life. For this reason, more sustainable lubricants are needed as a middle point between waste generation and tool life. Since 2001, Ionic Liquids (ILs) have attracted interest as high-performance lubricants and lubricant additives. In this work, the lubricating ability of one halogen-containing and two halogen-free ILs used as additives in water has been investigated and compared to a halogen-containing cutting fluid (CF). Tests were performed using a pin-on-disk tribometer for aluminum-tungsten carbide pair. The worn surfaces of the disks and balls were analyzed by optical and scanning electron microscopies, non-contact 3D profilometry and energy dispersive X-ray spectroscopy. It was found that the addition of 1 wt% of one of the halogen-free ILs reduces friction and wear of both aluminum disks and ceramic balls with respect to dry or water-lubricated conditions. In addition, no wear was detected on the ball surface, therefore increasing the tool life compared to the CF.